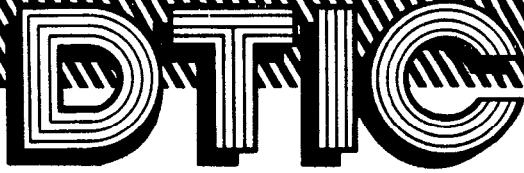


UNCLASSIFIED/UNLIMITED

6259

The logo for the Defense Technical Information Center (DTIC) is displayed in a large, stylized, outlined font. The letters 'D', 'T', 'I', and 'C' are interconnected and set against a background of diagonal hatching.

**NOTICE**

This document has been withdrawn from the DDC bulk storage. It is the responsibility of the recipient to promptly mark it to indicate the reclassification action shown herein.

# Technical Report

distributed by



**Defense Technical Information Center  
DEFENSE LOGISTICS AGENCY**

Cameron Station • Alexandria, Virginia 22314

UNCLASSIFIED/UNLIMITED

UNCLASSIFIED

AD 2 2 4 4 1 5

DEFENSE DOCUMENTATION CENTER

FOR

SCIENTIFIC AND TECHNICAL INFORMATION

CAMERON STATION, ALEXANDRIA, VIRGINIA

CLASSIFICATION CHANGED  
TO UNCLASSIFIED

FROM CONFIDENTIAL L  
RESTRICTED DATA

PER AUTHORITY LISTED IN

DDC TAB NO U64-101 RBno. 150

DATE 15 May 64



UNCLASSIFIED

**UNCLASSIFIED**

NOTICE: When government or other drawings, specifications or other data are used for any purpose other than in connection with a definitely related government procurement operation, the U. S. Government thereby incurs no responsibility, nor any obligation whatsoever; and the fact that the Government may have formulated, furnished, or in any way supplied the said drawings, specifications, or other data is not to be regarded by implication or otherwise as in any manner licensing the holder or any other person or corporation, or conveying any rights or permission to manufacture, use or sell any patented invention that may in any way be related thereto.

**UNCLASSIFIED**

UNCLASSIFIED

WT-918

Copy No. 116 A

# ASTLE

PRECIPITATED PROTONS

*scale 7*

.6b

## RADIOCHEMICAL ANALYSIS OF FALLOUT

15773  
MAY 20 1959  
RECORDED  
TISIA



defined in Section 1 of 1954  
Its transmittal or the disclosure of its  
contents in any manner to an unauthorized  
person is prohibited.

HEADQUARTERS FIELD COMMAND, ARMED FORCES SPECIAL WEAPONS PROJECT  
SANDIA BASE, ALBUQUERQUE, NEW MEXICO

UNCLASSIFIED

REPRODUCTION OF THIS DOCUMENT IS PROHIBITED  
EXCEPT BY AUTHORITY OF THE ARMY

**UNCLASSIFIED**

Reproduced directly from manuscript copy by  
AEC Technical Information Service Extension  
Oak Ridge, Tennessee

Inquiries relative to this report may be made to  
Chief, Armed Forces Special Weapons Project  
Washington, D. C.

If this report is no longer needed, return to  
AEC Technical Information Service Extension  
P. O. Box 401  
Oak Ridge, Tennessee

**UNCLASSIFIED**

(4) NA

(5) 245-150

56-3384

241

REG. NO. 15856

(18) DICA

(19)

WT/918

LOG. NO. 5168

This document consists of 60 pages

WDSIT \_\_\_\_\_

No. 116 of 235 copies, Series A

(13) - (14) NA

(20) S-RJ

(6) OPERATION CASTLE.

(21) NA

Project 2.8b.

# RADIOCHEMICAL ANALYSIS OF FALLOUT [U]

(1) NA

(2) NA

(7) NA

REPORT TO THE SCIENTIFIC DIRECTOR

(10) By

Robert C. Tompkins and  
Philip W. Krey.

(11) February 1956, (17) 60p.

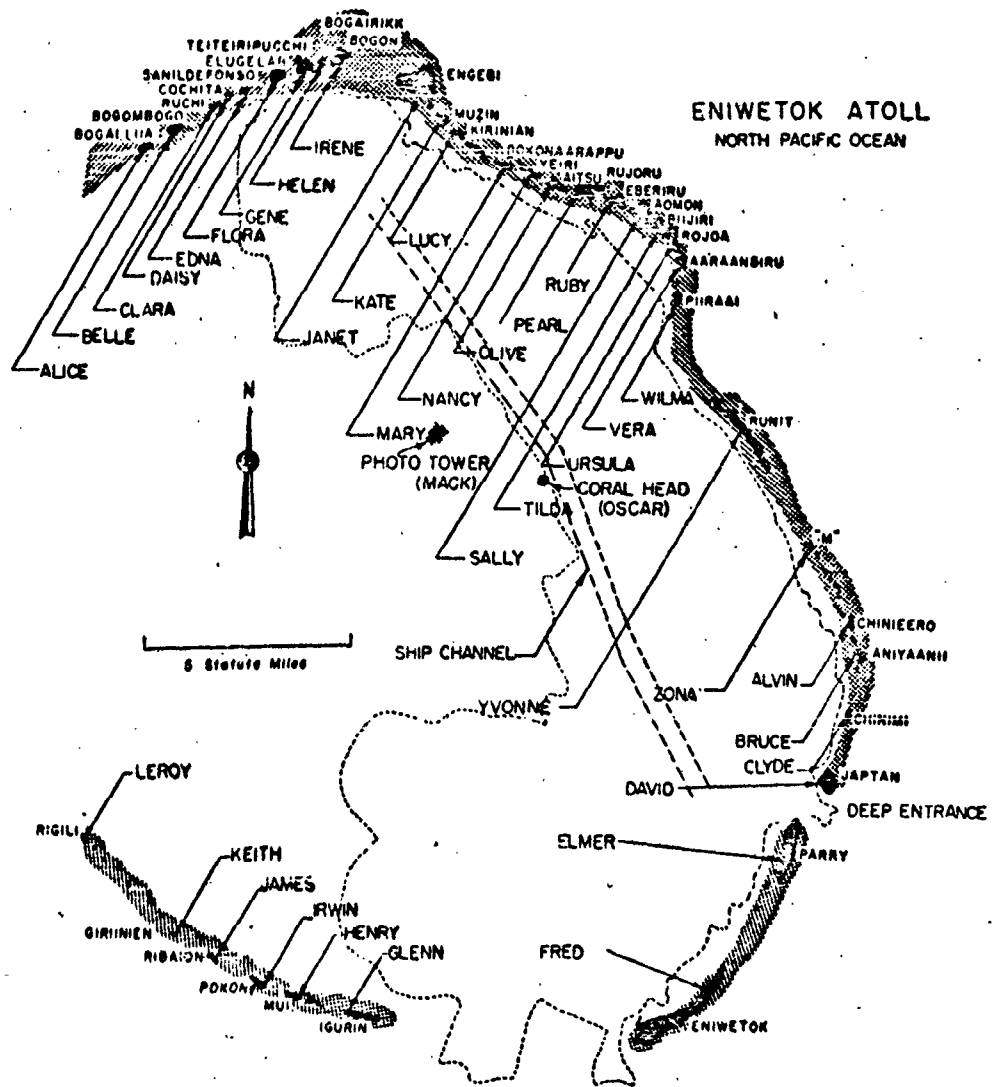
## RESTRICTED DATA

This document contains restricted data as defined in the Atomic Energy Act of 1954. Its transmittal or the disclosure of its contents in any manner to an unauthorized person is prohibited.

Chemical Corps  
Chemical and Radiological Laboratories  
Army Chemical Center, Maryland

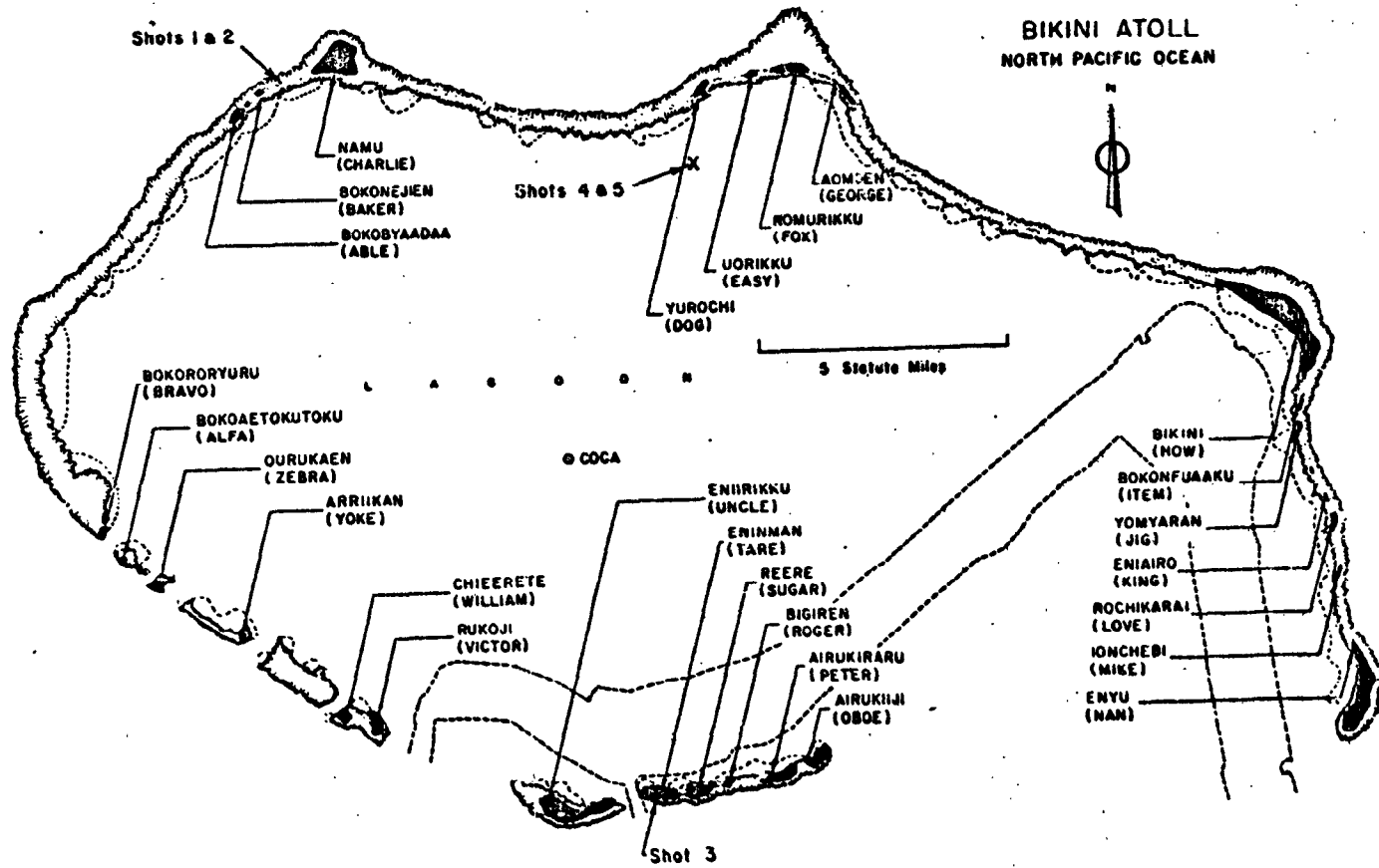
This document contains information affecting the National Defense of the United States within the meaning of the Espionage Laws, Title 18, U. S. C., Section 793 and in any manner to an unauthorized person is prohibited by law.

lgiv



SECRET - RESTRICTED DATA

3



GENERAL SHOT INFORMATION

	Shot 1	Shot 2	Shot 3	Shot 4	Shot 5	Shot 6
DATE	1 March	27 March	7 April	26 April	5 May	14 May
CODE NAME (Unclassified)	Bravo	Romeo	Koon	Union	Yankee	Nectar
TIME*	06:40	06:25	06:15	06:05	06:05	06:15
LOCATION	Bikini, West of Charlie (Namu) on Reef	Bikini, Shot 1 Crater	Bikini, Tara (Eninman)	Bikini, on Barge at Intersection of Arcs with Radius of 6900' from Dog (Yurochi) and 3 Statute Miles from Fox (Aomoen).		Eniwetok, IVY Mike Crater, Flora (Elugelab)
TYPE	Land	Barge	Land	Barge	Barge	Barge
HOLMES & NARVER COORDINATES	N 170,617.17 E 76,163.98	N 170,635.05 E 75,950.46	N 100,154.50 E 109,799.00	N 161,699.83 E 116,800.27	N 161,424.43 E 116,688.15	N 147,750.00 E 67,790.00

\* APPROXIMATE

SECRET - RESTRICTED DATA

\*\*\* is studied.

### ABSTRACT

~~The objectives of this project were to study the chemical and radiochemical composition of solid fallout as a function of particle size, zero-point environment, time and distance of collection, and gross decay characteristics, and to investigate the chemical and radiochemical nature of liquid fallout and base surge <sup>investigated</sup>.~~

A sample of solid fallout from Shot 1 was separated into 14 particle-size fractions which were analyzed for <sup>Sr-89, Zr-95, Mo-99, Ba-140,</sup> and ~~Ce-144~~. In each case the activity per unit weight of active particles below 50  $\mu$  was found to decrease regularly with increasing size, but in a different manner for each nuclide, indicating radiochemical fractionation. Above 50  $\mu$  the relationships were obscure. The gross decay did not vary at all with particle size at early times, and only slightly at later times.

In the fallout from Shots 1 and 3, <sup>Sr-89 and Ba-140</sup> showed a greater tendency to concentrate in the liquid phase than the other fission products studied.

Shot 4 fallout samples, principally liquid, obtained from a Project 2-5b intermittent fallout collector indicated that the relative concentrations of <sup>Sr-89 and Ba-140</sup> increase with time of collection.

~~The base surge sampling program was unsuccessful.~~

No information was obtained on variations of composition with distance. ←

\* Sr-89, Zr-95, Mo-99, Ba-140, and Ce-144

\*\* Sr-89 and Ba-140

## FOREWORD

This report is one of the reports presenting the results of the 34 projects participating in the Military Effects Tests Program of Operation CASTLE, which included six test detonations. For readers interested in other pertinent test information, reference is made to WT-934, Summary Report of the Commander, Task Unit 13, Programs 1-9, Military Effects Program. This summary report includes the following information of possible general interest.

- a. An over-all description of each detonation, including yield, height of burst, ground zero location, time of detonation, ambient atmospheric conditions at detonation, etc., for the six shots.
- b. Discussion of all project results.
- c. A summary of each project, including objectives and results.
- d. A complete listing of all reports covering the Military Effects Test Program.

## ACKNOWLEDGEMENTS

Many helpful suggestions for the planning of the project were made by the Director of Program 2, Lt Col E. A. Martell. Special credit is due J-3 Division, Task Group 7.1, for their splendid cooperation during the difficult recovery operation for Shot 1.

## CONTENTS

ABSTRACT. . . . .	5
FOREWORD. . . . .	7
ACKNOWLEDGMENT . . . . .	7
ILLUSTRATIONS . . . . .	11
TABLES . . . . .	11
CHAPTER 1 INTRODUCTION . . . . .	13
1.1 Objectives . . . . .	13
1.1.1 Purpose. . . . .	13
CHAPTER 2 THEORY AND BACKGROUND. . . . .	14
2.1 Theory. . . . .	14
2.2 Background. . . . .	15
CHAPTER 3 EXPERIMENT DESIGN. . . . .	16
3.1 Introduction. . . . .	16
3.2 Field Instrumentation . . . . .	16
3.2.1 Two-Phase Fallout Collector. . . . .	16
3.2.2 Intermittent Fallout Collector . . . . .	19
3.2.3 Laboratory Trailer. . . . .	19
3.2.4 Station Layout. . . . .	19
3.3 Operations . . . . .	20
3.3.1 General Procedure . . . . .	20
3.3.2 Summary of Shots . . . . .	20
3.3.2.1 Shot 1 . . . . .	20
3.3.2.2 Shot 2 . . . . .	20
3.3.2.3 Shot 3 . . . . .	20
3.3.2.4 Shot 4 . . . . .	22

3.4 Analytical Methods . . . . .	22
3.4.1 Particle Size Separation. . . . .	22
3.4.2 Preparation of Samples . . . . .	23
3.4.3 Radiochemistry. . . . .	23
3.4.4 Counting Techniques . . . . .	24
3.4.5 Quantitative Analysis . . . . .	26
3.4.6 Autoradiography . . . . .	27
CHAPTER 4 RESULTS . . . . .	28
4.1 Shot 1: Size-Graded Fallout From How. . . . .	28
4.2 Time-Differentiated Fallout. . . . .	32
4.3 Comparison of Liquid and Solid Activity. . . . .	33
4.4 Leaching Studies . . . . .	33
CHAPTER 5 DISCUSSION . . . . .	35
5.1 Discussion of Errors . . . . .	35
5.2 Evaluation of Size Separation and Autoradiograph . . . . .	37
5.3 Variation of Radiochemical Composition With Particle Size, Zero Point Environment, and Time and Distance of Collision . . . . .	40
5.4 Liquid Fallout and Base Surge. . . . .	44
5.5 Gross Decay . . . . .	44
CHAPTER 6 CONCLUSIONS AND RECOMMENDATIONS . . . . .	46
6.1 Conclusions . . . . .	46
APPENDIX A RADIOCHEMICAL PROCEDURES . . . . .	47
APPENDIX B CALIBRATION OF THE ROLLER ANALYZER . . . . .	51
APPENDIX C PERSONNEL ROSTER . . . . .	54
APPENDIX D EVALUATION OF TWO-PHASE COLLECTOR. . . . .	55
BIBLIOGRAPHY . . . . .	57

## ILLUSTRATIONS

3.1	Two-Phase Collector on Project 6.5 Barge in Eniwetok Lagoon.	17
3.2	Interior of Two-Phase Collector Showing Corked Delivery Tube.	17
3.3	Interior of Two-Phase collector with Chlorobenzene and Desiccant in Place. . . . .	18
3.4	Preparation of Two-Phase Collector on Janet for Shot 6. . . . .	21
3.5	Recovery of Total Fallout Samples (Janet) . . . . .	21
3.6	Ion Exchange Columns for Sodium Analysis . . . . .	24
3.7	Counting Equipment in Laboratory Trailer . . . . .	25
4.1	Per Cent Active Particles vs Particle Size. . . . .	29
5.1	Activity Concentration of Sr <sup>89</sup> vs Particle Size . . . . .	40
5.2	Activity Concentration of Zr <sup>95</sup> vs Particle Size . . . . .	41
5.3	Activity Concentration of Mo <sup>99</sup> vs Particle Size . . . . .	41
5.4	Activity Concentration of Ba <sup>140</sup> vs Particle Size. . . . .	42
5.5	Activity Concentration of Ce <sup>144</sup> vs Particle Size. . . . .	42
5.6	Gross Activity Concentration vs Particle Size. . . . .	43
5.7	Activity Concentration of Ca <sup>45</sup> vs Particle Size . . . . .	43
5.8	Negative Slope of Gross Decay vs Particle Size From 110-200 Days . . . . .	45
B.1	The Roller Analyzer . . . . .	52

## TABLES

3.1	Station Locations. . . . .	19
3.2	Two-Phase Collector Operation. . . . .	22
4.1	Per Cent Active Particles - Shot 1, How Station. . . . .	28
4.2	Activity Concentration of Size-Graded Fallout - Shot 1, How Station. . . . .	29
4.3	R-Values of Size-Graded Samples - Shot 1, How Station. . . . .	30
4.4	Activity and Particle Size Distribution of Total Fallout Sample From How Station, Shot 1. . . . .	31
4.5	Calcium Hydroxide Content of Fallout from Shot 1, How Station. . . . .	32
4.6	Time-Differentiated Fallout Shot 1, How Station. . . . .	32
4.7	R-Values of Time-Differentiated Fallout Shot 1, How Station. . . . .	32
4.8	Activity Concentration of Soil and Liquid Fallout. . . . .	33
4.9	Total Activity of Solid and Liquid Fallout Samples . . . . .	34
4.10	R-Values of Liquid and Solid Fallout. . . . .	34
5.1	Per Cent Spreads of All Radiochemical Analyses . . . . .	36
5.2	Predicted vs Observed Particle Size Separations by Standard Sieves. . . . .	38
5.3	Predicted vs Observed Particle Size Separations by Roller Analyzer. . . . .	38

# SECRET

## CHAPTER 1

### INTRODUCTION

#### 1.1 OBJECTIVES

The objectives of Project 2.6b were to determine:

1. The variations in chemical and radiochemical composition of solid fallout with particle size, zero-point environment, and time and distance of collection.
2. The chemical and radiochemical nature of liquid fallout and base surge, if formed.
3. The manner in which gross decay rates are affected by variations in radiochemical composition.

#### 1.1.1 Purpose

The purpose of obtaining these data was for use in studying basic problems of fallout phenomenology. The ultimate objective of this and similar work is to obtain data which may be used to develop a theory for the prediction of the military effects of operational nuclear weapons under specific conditions. Data obtained to meet the first objective may be used to aid in the development of a model of fireball dynamics in relation to particle formation. Liquid fallout was also studied to gain further insight into the history of the fallout material after its formation, and for documentation of internal radiation hazards. An investigation was carried out on the relation between decay rate and radiochemical composition because it appeared that it might be applicable to the problem of predicting the decay characteristics of fallout material from any operational detonation.

## CHAPTER 2

### THEORY AND BACKGROUND

#### 2.1 THEORY

The ultimate objective of studies in fallout phenomenology is the prediction of military effects from the operational use of nuclear weapons under any given field conditions.

The variables include:

1. Type and yield of weapon
2. Environment
  - a. Surface water
  - b. Underwater
  - c. Surface land
  - d. Underground
  - e. Soil type
  - f. Weather

In order to make these predictions it is necessary to have a general theory of the formation and subsequent history of fallout material. Such a theory must encompass several features.

First of all there must be a model of fireball dynamics, which determines the mechanism of formation of particles (or drops of water) and the distribution of the particles in the cloud.

The mechanism of particle formation for surface or subsurface detonations is more complicated than a simple vaporization and condensation of earth or water with the incorporation of fission products. There are a number of ways in which the activity may be associated with the particles. The activity may be deposited on the surfaces; it may be dispersed uniformly through the particle volume; or it may be dispersed in several non-uniform ways through the particle volume. Evidently, the mode of association is dependent upon the mechanism of particle formation and upon the subsequent history of the particles, which may produce changes such as agglomeration and leaching by water. The condensation process is not thoroughly understood and probably varies with different detonation surfaces. The factors which determine the particle size distribution of the condensate have not been established. In some cases, particularly underground shots, material may be thrown through the fireball without vaporization or even extensive fusion.

Radiochemistry provides a promising approach to the study of particle formation. The mode of association of activity with the particles is reflected in the relationship between activity (per particle or per unit mass) and particle size. Furthermore, since the different fission products have different chemical properties, and some have relatively long-lived gaseous precursors, they may become associated with the particles in different ways (fractionation). As a result different nuclides may exhibit, on radiochemical analysis, different relationships with particle size.

Other features such as transport and deposition of fallout involve meteorological conditions, which are beyond the scope of this project.

## 2.2 BACKGROUND

Radiochemical fractionation has been defined as any variation in the relative fission product nuclide abundance.<sup>1/</sup> The phenomenon was discovered at an early stage of atomic weapons testing when it was observed that certain fission product ratios vary with the type and location of sample.<sup>2,3/</sup> During the course of routine calculations of cascade impactor data from Operation GREENHOUSE,<sup>4/</sup> the authors discovered that gross fission product decay was related exponentially to particle size according to the equation,

$$NMD = ke^{fn},$$

where NMD is the number median diameter, n is the slope of the gross decay curve, and k and f are constants. It therefore appeared likely that radiochemical fractionation was primarily a function of particle size distribution in a sample.

Operation JANGLE afforded an opportunity to study fractionation in greater detail. Size-graded fallout from the underground shot was investigated radiochemically.<sup>5/</sup> The specific activity of several nuclides was found to vary regularly with particle size, in the range from 50 to 70  $\mu$ . Different nuclides were found to be distributed differently in the particles, e.g., Sr<sup>89</sup> on the surface and Zr<sup>95</sup> in the body of the particle. A theory was proposed based on the existence of gaseous precursors. Similar ideas have been discussed by Cadle<sup>6/</sup> and by Adams et al.<sup>7/</sup>

A similar investigation was undertaken at Operation IVY (Bouton et al.<sup>8/</sup>) for particles in the range from 70 to 220  $\mu$  for the study of a greater number of nuclides than at JANGLE. The analysis was seriously hampered by the presence of a large quantity of water in the fallout samples. Certain nuclides were selectively dissolved in significant amounts and contaminated the inactive particles. As a result no reliance could be placed on figures for the per cent active particles, which are necessary to correct the specific activities. For this reason the radiochemical data have thus far defied theoretical interpretation. They did suggest some strong possibilities, however. It appeared likely at the time that Mo<sup>99</sup>, like Sr<sup>89</sup>, was deposited on the surface of particles, possible as a result of the volatility of Mo<sup>03</sup> under the high temperatures associated with thermonuclear experiments.

## CHAPTER 3

### EXPERIMENT DESIGN

#### 3.1 INTRODUCTION

It was evidently necessary to correct in the Operation CASTLE studies some of the experimental difficulties experienced at IVY and to extend the scope of the investigation. In order to minimize the contamination of inactive particles by active solution and to avoid collection of excessive amounts of extraneous dust and rain, a new system was devised for collecting fallout, which is described below. The range of particle size under investigation was extended downward to 5  $\mu$ .

This operation provided three types of detonation: surface land, surface water, and intermediate. Unfortunately operational difficulties prevented an adequate comparison of effects from the different types. It was originally an objective of this project to study base surge, but the base surge collecting stations were destroyed, as reported by Wilsey and co-workers.<sup>9/</sup>

#### 3.2 FIELD INSTRUMENTATION

##### 3.2.1 Two-Phase Fallout Collector

This collector was essentially an inverted cone, 2 ft in diameter at the base, and 2 1/2 ft in height (Fig. 3.1). The cone was equipped with a dust-proof and water-tight cover which slid open when a signal was received, remained open for 5 hrs, and automatically slid shut. Approximately 4 liters of a solution of carbon tetrachloride in chlorobenzene (one part carbon tetrachloride to five parts chlorobenzene) were placed in the bottom of the collector. One liter of aqueous solution containing 0.5 per cent Aerosol OT and 0.125 per cent Versene was stored in a container mounted on the side of the collector. A delivery tube from this container extended into the collector and was stoppered with a cork connected to the cover of the collector (Fig. 3.2). When a signal was received, the cover opened retracting the cork from the delivery tube. The aqueous solution flowed onto the heavier, immiscible organic liquid. When fallout arrived at the collector, all

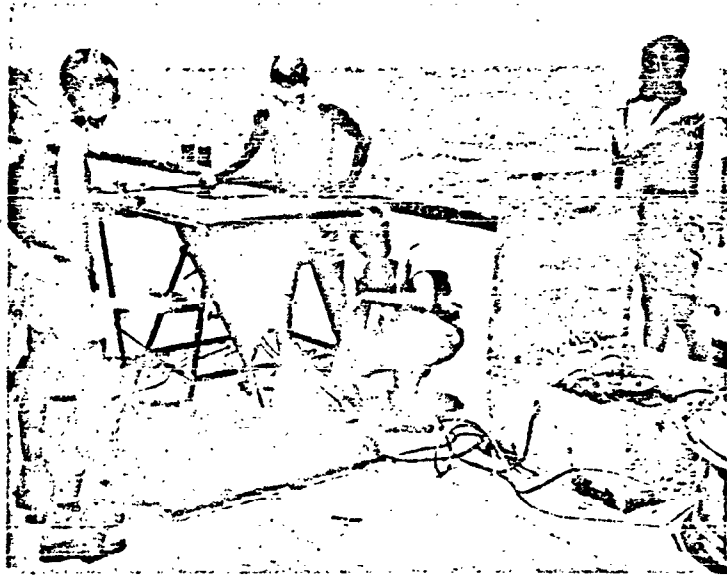


Fig. 3.1 Two-Phase Collector on Project 6.5 Barge in Eniwetok Lagoon

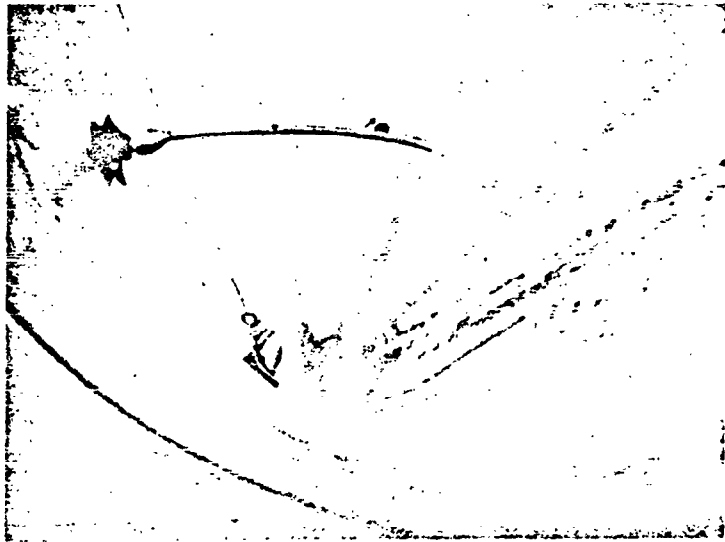


Fig. 3.2 Interior of Two-Phase Collector Showing Corked Delivery Tube

solid material sank into the organic phase, and liquid fallout remained in the aqueous phase. The Aerosol OT, a wetting agent, was used to lower the interfacial tension thereby permitting the solid particles to descend into the chlorobenzene solution. Versene is an agent used to preferentially complex any cations in the aqueous phase and to limit any distribution of the cations between the two phases. Carbon tetrachloride was used to minimize emulsification in the chlorobenzene. A bag of desiccant was placed in the chlorobenzene solution to absorb any moisture present in the organic phase. (Fig. 3.3)



Fig. 3.3 Interior of Two-Phase Collector with Chlorobenzene and Desiccant in Place

Since the efficiency of the collector was dependent upon the concentration of the wetting agent and complexing agent, a reservoir was mounted on the side of the collector to counteract the dilution of the aqueous phase by any rainfall that might occur during the collection period. This second container was equipped with a 4 1/2-in diameter funnel to which a condom was connected inside the container. If the rain fell into the collector, a comparable amount fell into the funnel, thereby swelling the condom. This would displace a 16 per cent Aerosol, 4 per cent Versene solution from the container into the collector, thus keeping the original concentrations in the aqueous phase constant. The mouth of the funnel was exposed only when the cover of the collector was open.

After Shot 1 the concentration of the Versena in the aqueous phase was changed to 1.75 per cent. The concentration of the reservoir solution was also changed to 10.7 per cent Aerosol OT and 4.7 per cent Versena.

A hand-controlled gate valve was located 9 1/4 in. above the bottom of the cone so that the aqueous phase could be easily drawn off. A quick-opening valve was located at the apex of the cone so that the solid material could be drawn off with the organic phase.

An evaluation of the collector operation is given in Appendix D.

### 3.2.2 Intermittent Fallout Collector

This instrument consists of a series of 24 trays which are exposed in turn to the fallout for any arbitrary period of time from 1 to 30 min. It was used in this project for the investigation of variations in radiochemical composition with time. A complete description can be found in the report of Project 2.5b. 10/

### 3.2.3 Laboratory Trailer

Analytical work at the test site was carried out primarily in the laboratory trailer, Radiac Sec AN/MDQ-1, obtained from the Signal Corps, which was set up on Parry Island, Eniwetok Atoll. A description is given in TM-11-5537.

### 3.2.4 Station Layout

Two-phase collectors were located as shown in Table 3.1.

TABLE 3.1 - Station Locations

Islands	Distance from Ground Zero (ft)		
	Shot 1	Shot 3	Shot 6
<u>Bikini Atoll</u>			
How	97,730		
Nan	122,230	69,280	
Victor	62,500	28,430	
Yoke	54,470	43,190	
Bravo	47,740	59,520	
Fox	50,600		
Oboe	83,660		
Tare	77,800		
<u>Eniwetok Atoll</u>			
Mack			47,700
Project 6.5 Barge			35,000
Janet			16,400
Mary			28,800

### 3.3 OPERATIONS

#### 3.3.1 General Procedure

The general scheme for preparation of the two-phase collectors was as follows:

1. The rain-displacement reservoir was filled with solution and adjusted so that addition of 1 drop of water to the funnel caused 1 drop of solution to flow into the collector.
2. The appropriate volume of chlorobenzene-carbon tetrachloride mixture was added together with the bag of desiccant, and the liquid level was measured.
3. After insertion of the cork and closure of the cover, the other reservoir was filled. (Fig. 3.4)

Recovery was made in conjunction with the recovery operation of Project 2.5b. The general scheme for the recovery of the total fallout samples was as follows:

1. Upon arrival at the station, the activity was recorded.
2. The cover of the two-phase collector was opened, abnormalities inside the collector were noted, and the liquid level was measured.
3. The valve on the side of the collector was opened, and all the aqueous phase collected in a suitable container.
4. After the aqueous phase was drawn off, the chlorobenzene phase along with the solid fallout was collected through the quick-opening valve at the bottom of the collector (Fig. 3.5).

#### 3.3.2 Summary of Shots

##### 3.3.2.1 Shot 1

The Shot 1 device was detonated on the reef of Bikini Atoll near Charlie at 0645 local time, 1 March 1954. Samples were recovered by helicopter on D+4 and D+5 and returned to Parry Island by destroyer. Analysis was begun on D+6. Only the How sample was suitable for particle size work. Samples from Victor and Fox were used for comparison of aqueous and solid phases. A crater sample was obtained from Task Unit 7.

##### 3.3.2.2 Shot 2

The Shot 2 device was detonated on a barge in the Shot 1 crater at 0630 local time, 27 March 1954. The two-phase collectors were not activated for this event. A ground sample from Able and liquid from the crater were obtained from Task Unit 7.

##### 3.3.2.3 Shot 3

The Shot 3 device was detonated on Tare at 0620 local time, 7 April 1954. Samples were recovered by helicopter on D+1 and returned to Parry Island by sea-going tug. Analysis was begun on D+3. Samples were obtained from Victor and Yoke, but were quite small on



Fig. 3.4 Preparation of Two-Phase Collector on Janet for Shot 6

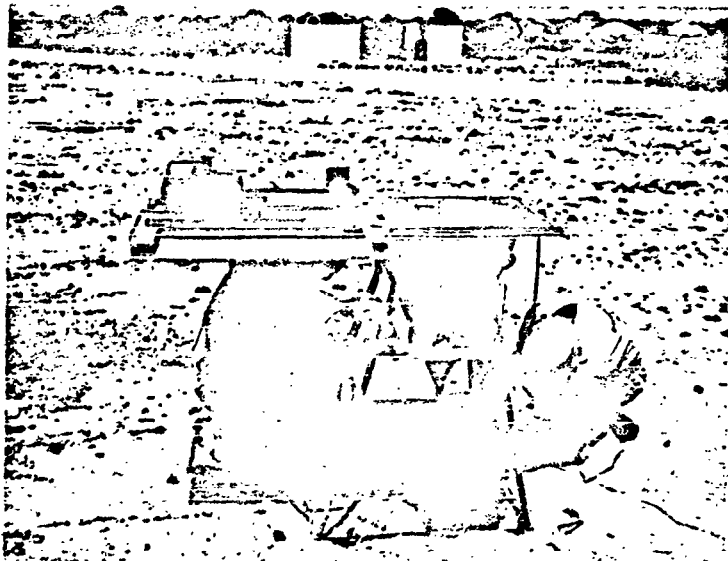


Fig. 3.5 Recovery of Total Fallout Samples (Janet)

account of the low yield of the device. A ground sample was obtained from George.

### 3.3.2.4 Shot 4

The Shot 4 device was detonated on a barge in the northern part of Bikini Lagoon at 0610 local time, 26 April 1954. The two-phase collectors were not activated for this event. Samples from the intermittent fallout collector on How were obtained from Project 2.5b.

This project did not participate in Shot 5. No satisfactory samples were obtained from Shot 6. A summary of collector operation is given in Table 3.2.

TABLE 3.2 Two-Phase Collector Operation

Station	Shot 1	Shot 3	Shot 6
How	Failed to Close		
Han	Satisfactory	Failed to close	
Victor	Satisfactory	Satisfactory	
Yoke	Damaged by flying debris		
Bravo	Failed to Close	Triggered before shot	
Fox	Satisfactory		
Osce	Did not operate; electrical failure		
Tare	Did not operate; electrical failure		
Meek			Did not operate
Project 6.5			Motor burned out before shot on account of shot 1 damage
Barge			Satisfactory
Janet			Satisfactory
Pary			Satisfactory

## 3.4 ANALYTICAL METHODS

### 3.4.1 Particle Size Separation

In order to meet the first objective of this project, it was necessary to size grade the sample in such a manner as to provide a sufficient quantity in each size range to perform the required analyses. For this reason it was decided to use standard sieves down to the smallest particle size possible and the Roller analyzer below that point. The limitations of these techniques are discussed in Section 5.2.

The mixture of solid fallout and approximately 50 ml of the chlorobenzene from the two-phase collector was slurried on a 44  $\mu$  sieve and permitted to settle through the sieve. This procedure was repeated three times. The sieve was then tilted and the chlorobenzene solution that had settled through the sieve was re-added with a dropping pipette so that the solution settled through an exposed section of the sieve. When all the particles were washed to one side of the sieve, the sieve was tilted in the other direction and the process repeated. Care was exercised to keep one section of the sieve clear of large particles

so that the small particles in the wash could settle through without being blocked by large particles.

The particles remaining on the sieve were washed with approximately 20 ml of acetone and dried. These particles were then placed in the Roller analyzer; all particles below 40  $\mu$  in diameter were blown over into an asbestos collection thimble. This step greatly reduced the number of fines in the larger particle sizes. These large particles were then sieved dry with mechanical shaking for 5 min into 9 size-fractions.

The small particles that had settled with the chlorobenzene through the 44  $\mu$  sieve were centrifuged, washed with approximately 20 ml of acetone, and dried. They were combined with the fraction below 40  $\mu$  that had been separated by the Roller analyzer. (see Appendix B) This entire sample was then separated by the Roller analyzer into 5 size-fractions.

Particle sizes are reported as mean volume diameters:

$$d_v = \sqrt[3]{\frac{\sum n_i d_i^3}{\sum n_i}}$$

### 3.4.2 Preparation of Samples

The various fractions of the size-graded fallout were weighed, dissolved in 5 ml of conc. nitric acid, and heated to insure complete dissolution. Aliquots of the aqueous phases were fumed to dryness twice with concentrated nitric acid and then with a mixture of nitric and perchloric acids. The final solutions were made up to volume with water. Aliquots of all solutions were measured for gross activity and decay. Other liquid and solid samples were treated in a similar manner.

For the leaching studies a weighed quantity of the solid fallout was placed in a sintered glass crucible and slurried with 10 ml of water for 10 min. The mixture was filtered through the crucible and the filtrate diluted to volume. The crucible was dried at 110°C for 30 min, cooled, and weighed to determine the weight of sample removed by the leaching. Subsequent leaches were carried out with dilute hydrochloric acid which permitted greater dissolution of the particles.

### 3.4.3 Radiochemistry

$\text{Na}^{24}$  and  $\text{Mo}^{99}$  analyses were performed at the test site;  $\text{Ca}^{45}$ ,  $\text{Fe}^{59}$ ,  $\text{Sr}^{89}$ ,  $\text{Zr}^{95}$ ,  $\text{Ba}^{140}$ , and  $\text{Ce}^{144}$  analyses were performed at the Army Chemical Center. Four aliquots of each sample were taken for each analysis except in the case of the  $\text{Na}^{24}$  procedure where only one aliquot was analyzed. The reported results are the averages of the four aliquots.

The separation procedure for  $\text{Cr}^{89}$  and  $\text{Ba}^{140}$  is essentially that of Glendenin. 11/ The only significant modification is that the barium is finally precipitated and mounted as the chromate. The procedures for  $\text{Zr}^{95}$ ,  $\text{Mo}^{99}$ , and  $\text{Ce}^{144}$  are the methods employed by the Radiochemistry Group J-11, Los Alamos Scientific Laboratory. 12/ The  $\text{Na}^{24}$  and  $\text{Ca}^{45}$  analyses were developed by these Laboratories and are

described in Appendix A. The ion exchange columns used for the  $\text{Na}^{24}$  analyses are shown in Fig. 3.6. Determinations of  $\text{Fe}^{59}$  activities

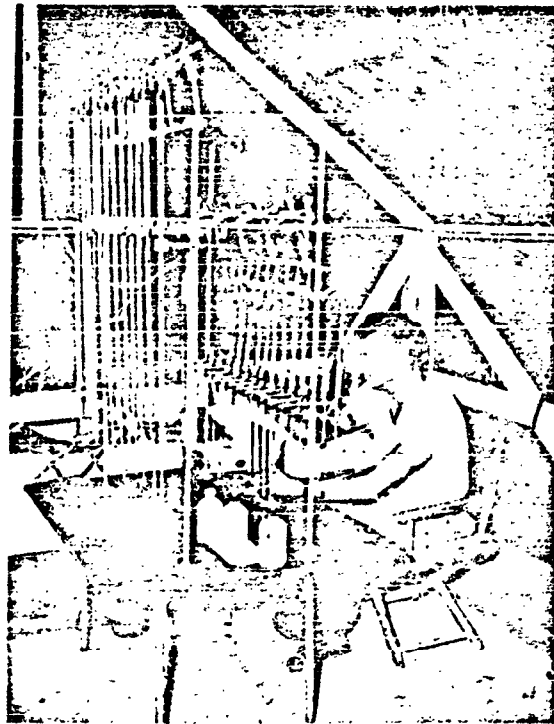


Fig. 3.6 Ion Exchange Columns for Sodium Analysis

were attempted by gamma ray spectrometric analyses. All radiochemical samples were mounted in the center of  $2\frac{1}{2} \times 3\frac{1}{2}$  in. aluminum cards and covered with  $0.45 \text{ mg/cm}^2$  plicofilm.

#### 3.4.4 Counting Techniques

Counting was carried out with thin mica window GM counters mounted on Lucite stages. These stages were of the same basic design as the commercial models such as RCL Mk 4, Model I, modified by these Laboratories to provide an absorber shelf and to improve reproducibility of counter positioning. The stages and counters were housed in Technical Associates Model LS2 vertical lead pigs. Output was fed to Berkely 2000 scalars. The counting room in the laboratory trailer is shown in Fig. 3.7.

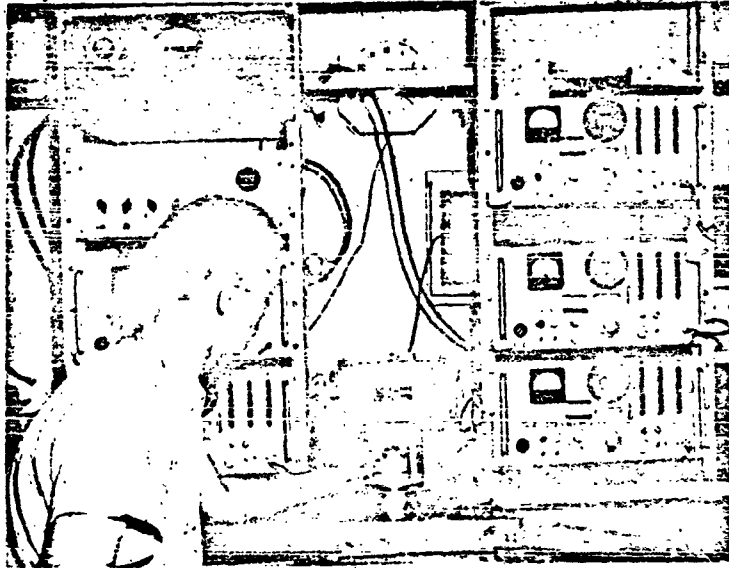


Fig. 3.7 Counting Equipment in Laboratory Trailer

Every sample was counted for a total of 10,000 counts or for a total counting time of 30 min, whichever occurred first. The former provided for a 0.95 error of 2 per cent (i.e., a 95 per cent probability of being within 2 per cent of the true counting rate), but a time restriction was necessary because of the work load. The background was continuously monitored with a General Radio count rate meter to indicate any severe variations in the background which would invalidate the counting done at that time. Counting rates in excess of 5000 c/m were corrected for coincidence loss.

Standards of each fission product of interest were separated from a sample of  $U^{235}$  irradiated with thermal neutrons in the Brookhaven reactor. These standards were used for three purposes:

1. Cross-calibration of counters for each shelf position. New counters placed in service later in the operation were cross-calibrated by means of fission products separated from the fallout samples.

2. Ratios for the standardization of R-values. (R-values are obtained by dividing the observed ratio of two nuclides in a shot sample, corrected to zero time, by the activity ratio of the same two nuclides for thermal neutron fission of  $U^{235}$  counted under the same conditions.)

3. Conversion of counting rates to microcuries. Although the primary interest of this project was in relative activities, advantage was taken of these standards to calculate absolute activities. Since the neutron flux, weight of  $U^{235}$ , and fission yields 17/ were known, it was possible to obtain for each fission product of interest a ratio of  $\mu\text{c}$  to  $\text{c/m}$  for each counter. The fission cross section of  $U^{235}$  was taken as 575 barns.

Except in the case of very long lived nuclides, counting rates were read from smoothed decay curves. These values were corrected to zero time, 100 per cent chemical yield, zero added absorber, and standard tube and shelf.

The corrections to zero added absorber were based upon absorption curves measured in these Laboratories. Data for  $Ca^{45}$  and  $Mo^{99}$  were corrected for self-absorption and self-scattering. The errors introduced by neglecting these corrections for  $Sr^{89}$ ,  $Zr^{95}$ ,  $Ba^{140}$ ,  $Ca^{141}$  are discussed in Section 5.1. The aluminum cards on which the samples were mounted provided infinite back-scattering.

For the gross activity measurements small aliquots of the dissolved samples were evaporated in glass counting cups. The counting technique was similar to that for the individual nuclides except that the various corrections were not attempted.

Gross decay measurements from 110 to 200 days were performed on aliquots of the dissolved size fractions evaporated in small glass planchets. The counting was done with thin mica end window GM counters. The physical geometry of the system was defined by a hole in a  $3/8$  inch brass plate which minimized the contribution of side scattering. The total absorption between the sample and the sensitive volume of the counter corresponded to about  $6 \text{ mg/cm}^2$ . The counting rates were corrected only for coincidence loss. Since absorption and scattering effects are more or less significant depending upon the beta energies, the slopes of the gross decay curves cannot be directly correlated with the radiochemical composition unless these pertinent corrections have been made.

#### 3.4.5 Quantitative Analysis

As a result of the tremendous heat generated by the detonations, large volumes of sea water were evaporated and sodium chloride was incorporated into the fireball. Bunney and Ballou 13/ concluded from a thermodynamic study that chloride ion would be the predominant form of chlorine in the fallout. They reasoned that the strong electro-negativity of chlorine would cause it to react at high temperature with alkali and some other metals to form chlorides. They do not consider chlorates and perchlorates possible at high temperature. For further information with regard to formation of the particles in the fireball and their subsequent history, the chloride ion concentration was determined by the Volhard method 14/ in each size-fraction of the fallout.

The calcium ion concentration for each size-fraction of the fallout was also determined by the method described by Treadwell and Hall 15/. This procedure involves the quantitative precipitation of

the calcium as the oxalate and then the titrimetric determination of the oxalate with potassium permanganate.

The surface water shots vaporized the 250 ton steel barges upon which the devices were detonated. The concentration of iron was measured in the fallout from these shots by a colorimetric determination of the intense red complex formed by ferrous ion and o-phenanthroline. 16/

#### 3.4.6 Autoradiography

Portions of size-graded sample fractions were studied autoradiographically. Each fraction was monitored to estimate its radioactivity, then deposited on Nuclear Track Beta stripping film and exposed for a time estimated to give good contrast between radioactivity-affected film areas and background areas. The developed autoradiograph was examined by microprojection to measure the particles and determine if they were radioactive. This yielded gross size distribution, radioactive to total particle ratio, and where their number was statistically sufficient, radioactive particles size distribution.

The per cent active particle data were calculated on a volume basis:

$$\% \text{ Active} = \frac{(\sum n_i d_i)^3}{(\sum n_i d_i)^3_{\text{total}}} \text{ active} \times 100$$

The detailed technique is described in the report of Project 2.5b.

CHAPTER 4

RESULTS

4.1 SHOT 1: SIZE-GRADED FALLOUT FROM HOW

In order to obtain activity per unit weight of active particles only, correction must be made for the per cent of inactive particles in the sample. The values for per cent active particles (by volume) obtained from the autoradiographs are listed in Table 4.1 along with

TABLE 4.1 Per Cent Active Particles - Shot 1, How Station

Particle Size in $\mu$	Observed Per Cent Active Particles	Per Cent Active Particles from Smooth Curve
5.08	4.16	4.16
10.3	63.7	11.3
23.3	36.5	35.8
29.5	48.5	49.6
43.7	84.8	84.8
62.4	95.3	86.8
70.5	84.5	86.8
85.8	75.8	86.8
113	91.6	86.8
116	75.4	86.8
172	79.9	86.8
215	96.8	86.8
239	96.9	86.8

the values read from the smooth curve (Fig 4.1). Table 4.2 lists the activity concentrations (activity per unit weight of fallout) of  $\text{Ca}^{45}$ ,  $\text{Sr}^{89}$ ,  $\text{Zr}^{95}$ ,  $\text{Mo}^{99}$ ,  $\text{Ba}^{140}$  and  $\text{Ce}^{144}$  and the gross activity concentrations for the various size fractions corrected for per cent active particles. Data on  $\text{Na}^{24}$  are not included because  $\text{Na}^{24}$  samples were contaminated with  $\text{Ba}^{140}$ . When it was learned that the shot device contained sodium tracer, it did not appear worthwhile to undertake the task of resolving the decay curves.

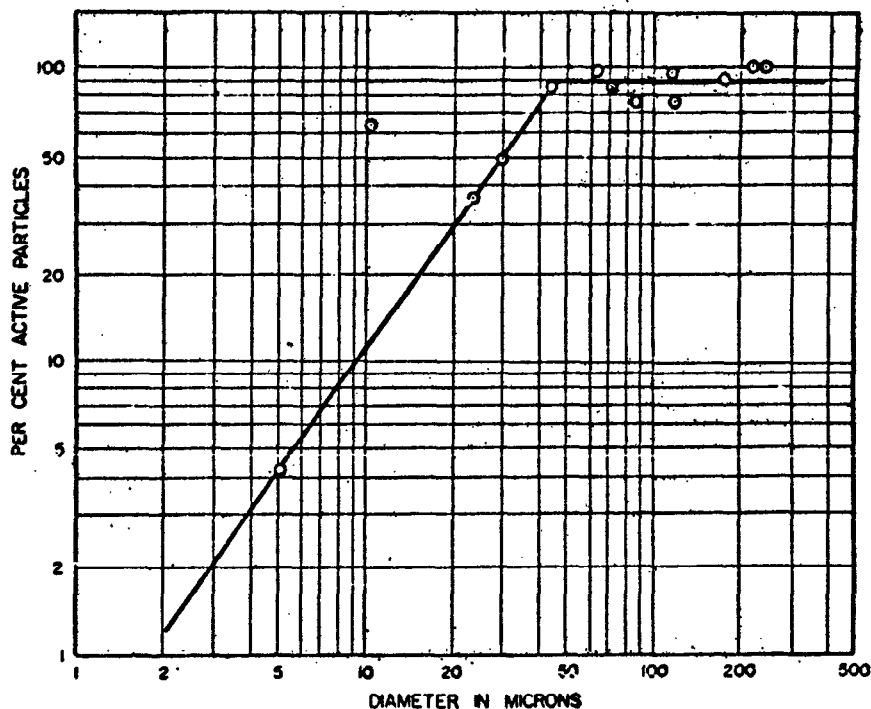


Fig. 4.1 Per Cent Active Particles vs Particle Size

TABLE 1.2  $Ca^{45}$  Activity Concentrations of Size-Graded Fallout - Shot 1, How Station

$d_p$ in $\mu$	Activity Concentration in $\mu\text{e}/\text{mg}$ of Hot Particles at Zero Time					Gross Activity Concentration of Hot Particles in Arbitrary Units at D+7 Days	$Ca^{45}$ Concentration of Particles in Arbitrary Units
	$Sr^{90}$	$Zr^{95}$	$Mo^{99}$	$Ag^{110}$	$Ca^{44}$		
5.08	$1.26 \times 10^{-1}$	$3.08 \times 10^{-1}$	14.9	2.70	$7.62 \times 10^{-2}$	60.6	29.1
10.3	$3.36 \times 10^{-2}$	$1.25 \times 10^{-1}$	7.00	$8.22 \times 10^{-1}$	$3.42 \times 10^{-2}$	20.8	21.8
20.3	$1.56 \times 10^{-2}$	$5.78 \times 10^{-2}$	2.88	$2.33 \times 10^{-1}$	$1.23 \times 10^{-2}$	8.04	9.83
29.5	$7.58 \times 10^{-3}$	$4.17 \times 10^{-2}$	2.02	$1.68 \times 10^{-1}$	$9.94 \times 10^{-3}$	5.74	9.27
43.7	$4.28 \times 10^{-3}$	$3.61 \times 10^{-2}$	1.20	$8.59 \times 10^{-2}$	$6.65 \times 10^{-3}$	4.69	7.45
62.4	$5.60 \times 10^{-3}$	$2.58 \times 10^{-2}$	1.78	$9.55 \times 10^{-2}$	$5.50 \times 10^{-3}$	3.61	1.21
70.5	$5.91 \times 10^{-3}$	$3.32 \times 10^{-2}$	1.75	$9.85 \times 10^{-2}$	$4.92 \times 10^{-3}$	2.96	4.06
85.8	$6.34 \times 10^{-3}$	$3.22 \times 10^{-2}$	1.59	$1.08 \times 10^{-1}$	$5.78 \times 10^{-3}$	3.33	7.70
113	$6.32 \times 10^{-3}$		1.47	$1.03 \times 10^{-1}$	$4.92 \times 10^{-3}$	2.68	2.57
116	$7.15 \times 10^{-3}$		1.50	$1.12 \times 10^{-1}$	$4.69 \times 10^{-3}$	2.59	3.50
172	$6.99 \times 10^{-3}$		1.49	$1.00 \times 10^{-1}$	$4.35 \times 10^{-3}$	2.60	
215			1.47	$9.42 \times 10^{-2}$	$3.88 \times 10^{-3}$	2.33	
239	$6.62 \times 10^{-3}$		1.27	$1.27 \times 10^{-1}$	$3.78 \times 10^{-3}$	2.33	
>300	$2.63 \times 10^{-3}$		0.931	$5.07 \times 10^{-2}$	$1.52 \times 10^{-3}$	0.754	

Table 4.3 lists the R-values, standardized by use of data from thermal neutron bombardment of U<sup>235</sup> in the Brookhaven reactor. The

TABLE 4.3 R-Values of Size-Graded Samples - Shot 1, How Station

d in $\mu$	R-Value			
	$\frac{Sr^{89}}{Mo^{99}}$	$\frac{Zr^{95}}{Mo^{99}}$	$\frac{Ba^{140}}{Mo^{99}}$	$\frac{Ca^{144}}{Mo^{99}}$
5.08	$20.3 \times 10^{-2}$	$3.34 \times 10^{-1}$	$8.12 \times 10^{-1}$	$6.10 \times 10^{-1}$
10.3	$11.5 \times 10^{-2}$	$3.88 \times 10^{-1}$	$5.24 \times 10^{-1}$	$5.84 \times 10^{-1}$
23.3	$8.92 \times 10^{-2}$	$4.39 \times 10^{-1}$	$3.65 \times 10^{-1}$	$5.14 \times 10^{-1}$
29.5	$9.00 \times 10^{-2}$	$4.50 \times 10^{-1}$	$3.75 \times 10^{-1}$	$5.92 \times 10^{-1}$
43.7	$8.55 \times 10^{-2}$	$6.53 \times 10^{-1}$	$3.21 \times 10^{-1}$	$6.66 \times 10^{-1}$
62.4	$7.56 \times 10^{-2}$	$3.16 \times 10^{-1}$	$2.41 \times 10^{-1}$	$3.69 \times 10^{-1}$
70.5	$7.99 \times 10^{-2}$	$4.13 \times 10^{-1}$	$2.54 \times 10^{-1}$	$3.37 \times 10^{-1}$
85.8	$9.63 \times 10^{-2}$	$4.45 \times 10^{-1}$	$3.07 \times 10^{-1}$	$4.38 \times 10^{-1}$
113	$10.4 \times 10^{-2}$		$3.16 \times 10^{-1}$	$4.03 \times 10^{-1}$
116	$11.5 \times 10^{-2}$		$3.37 \times 10^{-1}$	$3.76 \times 10^{-1}$
172	$9.87 \times 10^{-2}$		$3.04 \times 10^{-1}$	$3.52 \times 10^{-1}$
215			$2.89 \times 10^{-1}$	$3.18 \times 10^{-1}$
239	$12.6 \times 10^{-2}$		$4.49 \times 10^{-1}$	$3.59 \times 10^{-1}$
300	$7.61 \times 10^{-2}$		$2.75 \times 10^{-1}$	$2.20 \times 10^{-1}$

R-value is obtained by dividing the observed counting rate ratio of two nuclides at zero time by the corresponding ratio for a standard fission sample counted under the same conditions. Table 4.4 lists the weight, total activity, and gross decay exponents of one size fraction.

The samples contained less than 1 per cent Cl<sup>-</sup>. It was realized late in the operation that chloride was lost from the samples by heating with nitric acid. However the same result was obtained when the analysis was run on a portion of 1 size fraction dissolved at room temperature under non-oxidizing conditions. Analyses for Fe<sup>++</sup> indicated less than 0.076 per cent. Quantitative analyses for Ca<sup>++</sup> were used in conjunction with the total sample weights to calculate the Ca(OH)<sub>2</sub> content of the size-graded samples. The results are given in Table 4.5. The two particle sizes having the highest Ca(OH)<sub>2</sub> content are the same sizes which cannot be obtained in significant quantity by grinding coral in a mortar. No Fe<sup>59</sup> was detected with the gamma-ray spectrometer.

TABLE 4.4 Activity and Particle Size Distribution of Total Fallout Sample From How Station, Shot 1

Particle Size in $\mu$	Weight in g	Per Cent of Total Weight	Gross Activity in Arbitrary Units at D+7 Days	Per Cent of Total Activity	Slope of Log-Log Gross Decay Curve D+5 to D+30	Slope of Log-Log Gross Decay Curve D+110 to D+170
5.08	2.901	0.47	7.31	17.8	-2.0	-1.32
10.3	0.975	3.19	2.29	5.59	-2.0	-1.20
23.3	0.112	0.366	0.323	0.788	-2.0	-1.31
29.5	0.923	3.02	2.45	5.98	-2.0	-1.09
43.7	0.597	1.95	1.96	4.78	-2.0	-1.13
62.4	1.031	3.36	3.22	7.86	-2.0	-1.09
70.5	0.522	1.71	1.30	3.17	-2.0	-1.15
85.8	0.400	1.31	1.16	2.83	-2.0	-1.14
113	0.408	1.33	0.950	2.32	-2.0	-1.22
116	0.646	2.11	1.45	3.54	-2.0	-1.17
172	0.691	2.26	1.56	3.81	-2.0	-1.15
215	0.757	2.47	1.58	3.96	-2.0	-1.18
239	0.983	3.21	1.98	4.83	-2.0	-1.18
300	19.662	48.2	13.1	32.9	-1.8	-1.20
Total	30.608	100	41.0	100		

TABLE 4.5 Calcium Hydroxide Content of Fallout from Shot 1, How Station

Particle Sizes in $\mu$	Per Cent Ca(OH) <sub>2</sub>
5.08	11.1
10.3	40.7
23.3	100
29.5	16.0
43.7	28.1
62.4	37.2
70.5	12.2
85.8	15.4
113	12.8
116	26.3
172	23.6
215	16.8
239	12.6

#### 4.2 TIME-DIFFERENTIATED FALLOUT

Six liquid samples were made by combining several samples obtained over 30 min periods by the intermittent fallout collector on How (Shot 4, Project 2.5b). These samples contained little solid. Fission product activities and milligrams of Fe++ per milliliter of fallout are given in Table 4.6. R-values are given in Table 4.7. No dry samples were obtained.

TABLE 4.6 Time-Differentiated Fallout  
Shot 4, How Station

Time (After Shot) of sample Collection in hr	Activity in $\mu\text{c/ml}$ of Fallout at Zero Time				Fe++ in mg/ml
	Sr <sup>89</sup>	Y <sup>90</sup>	Ba <sup>140</sup>	Ce <sup>144</sup>	
1.5 - 3	$2.60 \times 10^{-3}$	$8.91 \times 10^{-2}$	$1.56 \times 10^{-2}$	$3.6 \times 10^{-4}$	$5.3 \times 10^{-3}$
3.5 - 5	$4.98 \times 10^{-3}$	$1.04 \times 10^{-1}$	$3.78 \times 10^{-2}$		$6.4 \times 10^{-2}$
8 - 9	$4.43 \times 10^{-3}$	$1.98 \times 10^{-1}$	$2.89 \times 10^{-2}$	$7.60 \times 10^{-4}$	$3.5 \times 10^{-3}$
9 - 10	$1.61 \times 10^{-3}$	$2.47 \times 10^{-2}$	$8.41 \times 10^{-3}$	$1.35 \times 10^{-4}$	$1.4 \times 10^{-3}$
10 - 11	$2.19 \times 10^{-3}$	$2.91 \times 10^{-2}$	$9.29 \times 10^{-3}$	$7.6 \times 10^{-5}$	$1.7 \times 10^{-3}$
11 - 12	$5.66 \times 10^{-3}$	$7.56 \times 10^{-2}$	$2.87 \times 10^{-2}$	$2.2 \times 10^{-3}$	$8.0 \times 10^{-2}$

TABLE 4.7 R-Values of Time-Differentiated  
Fallout Shot 4, How Station

Time (After Shot) of Sample Collection in hr	R-Values		
	Sr <sup>89</sup> /Y <sup>90</sup>	Ba <sup>140</sup> /Y <sup>90</sup>	Ce <sup>144</sup> /Y <sup>90</sup>
1.5 - 3	0.702	0.788	0.49
3.5 - 5	1.15	1.64	
8 - 9	0.538	0.661	0.462
9 - 10	1.56	1.53	0.656
10 - 11	1.81	1.43	0.31
11 - 12	1.80	1.71	3.6

#### 4.3 COMPARISON OF LIQUID AND SOLID ACTIVITY

Table 4.8 lists the activity concentration of Solid and liquid fallout samples. Activities per milliliter are not included for Shot 1 because evaporation made it impossible to determine the volume of liquid collected. Unless otherwise stated they are from the two-phase collector. The emulsion from Shot 3 was a mixture of chlorobenzene and water; its activity was shown to come from the liquid fallout. Table 4.9 lists the corresponding total activities. R-values are given in Table 4.10.

#### 4.4 LEACHING STUDIES

Leaching studies were abandoned after it was found by independent experiment that readsorption of activity from the leach solution makes it impossible to interpret the results.

TABLE 4.8 Activity Concentrations of Solid and Liquid Fallout

Fallout Sample	Activity in $\mu\text{e}$ at Zero Time				
	Sr <sup>89</sup>	Zr <sup>95</sup>	Mo <sup>99</sup>	Ba <sup>140</sup>	Ce <sup>144</sup>
<u>Shot 1</u>					
Fox solid	$2.41 \times 10^{-3}/\text{mg}$	$5.45 \times 10^{-3}/\text{mg}$	$2.51 \times 10^{-1}/\text{mg}$	$3.27 \times 10^{-2}/\text{mg}$	$1.82 \times 10^{-3}/\text{mg}$
Victor solid	$8.74 \times 10^{-4}/\text{mg}$	$1.12 \times 10^{-2}/\text{mg}$	$5.03 \times 10^{-1}/\text{mg}$	$2.61 \times 10^{-2}/\text{mg}$	$1.65 \times 10^{-3}/\text{mg}$
Crater solid	$4.9 \times 10^{-5}/\text{mg}$	$1.73 \times 10^{-4}/\text{mg}$	$7.41 \times 10^{-4}/\text{mg}$	$2.38 \times 10^{-4}/\text{mg}$	
Crater liquid	$2.00 \times 10^{-3}/\text{ml}$			$1.30 \times 10^{-2}/\text{ml}$	
<u>Shot 2</u>					
Crater liquid	$2.02 \times 10^{-3}/\text{ml}$		$2.93 \times 10^{-1}/\text{ml}$		
Able solid	$1.72 \times 10^{-4}/\text{mg}$		$5.49 \times 10^{-1}/\text{ml}$	$9.82 \times 10^{-4}/\text{mg}$	$3.70 \times 10^{-3}/\text{mg}$
<u>Shot 3</u>					
Victor solid	$4.44 \times 10^{-4}/\text{mg}$	$5.85 \times 10^{-3}/\text{mg}$	$6.9 \times 10^{-2}/\text{mg}$	$9.13 \times 10^{-4}/\text{mg}$	$5.19 \times 10^{-4}/\text{mg}$
Victor aqueous	$3.85 \times 10^{-3}/\text{ml}$	$3.66 \times 10^{-3}/\text{ml}$	$8.78 \times 10^{-3}/\text{ml}$	$7.98 \times 10^{-3}/\text{ml}$	$8.55 \times 10^{-4}/\text{ml}$
Victor emulsion	$3.21 \times 10^{-4}/\text{ml}$	$1.3 \times 10^{-4}/\text{ml}$	$1.12 \times 10^{-2}/\text{ml}$	$5.94 \times 10^{-4}/\text{ml}$	

TABLE 4.9 Total Activity of Solid and Liquid  
Fallout Samples

Sample	Activity in $\mu\text{c}$ at Zero Time				
	Sr <sup>89</sup>	Zr <sup>95</sup>	Mo <sup>99</sup>	Ba <sup>140</sup>	Ce <sup>144</sup>
<u>Shot 1</u>					
Fox solid	$3.48 \times 10^{-1}$	$7.90 \times 10^{-1}$	$3.63 \times 10^1$	4.72	$2.62 \times 10^{-1}$
Fox aqueous	1.04	1.82	$7.39 \times 10^1$	10.2	
Victor solid	$8.35 \times 10^{-1}$	10.7	$4.81 \times 10^2$	25.0	1.58
Victor aqueous		$3.69 \times 10^{-1}$	$2.84 \times 10^2$		
<u>Shot 2</u>					
Able solid	$1.75 \times 10^{-1}$		$5.59 \times 10^2$	$9.98 \times 10^{-1}$	3.76
Able leach			$9.37 \times 10^1$		
<u>Shot 3</u>					
Victor solid	$7.50 \times 10^{-2}$	$9.87 \times 10^{-1}$	$1.17 \times 10^1$	$1.55 \times 10^{-1}$	$8.80 \times 10^{-2}$
Victor aqueous	1.62	1.54	3.69	3.36	$3.60 \times 10^{-1}$
Victor emulsion	$8.36 \times 10^{-1}$	$3.4 \times 10^{-1}$	$2.92 \times 10^1$	1.54	

TABLE 4.10 R-Values of Liquid and Solid Fallout

Sample	R-Values			
	Sr <sup>89</sup> /Mo <sup>99</sup>	Zr <sup>95</sup> /Mo <sup>99</sup>	Ba <sup>140</sup> /Mo <sup>99</sup>	Ce <sup>144</sup> /Mo <sup>99</sup>
<u>Shot 1</u>				
Fox solid	$2.31 \times 10^{-1}$	$4.73 \times 10^{-1}$	$5.85 \times 10^{-1}$	$8.68 \times 10^{-1}$
Fox aqueous	$3.39 \times 10^{-1}$	$5.36 \times 10^{-1}$	$6.23 \times 10^{-1}$	
Victor solid	$4.17 \times 10^{-2}$	$4.87 \times 10^{-1}$	$2.34 \times 10^{-1}$	$3.94 \times 10^{-1}$
Victor aqueous		$2.85 \times 10^{-1}$	1.51	
Crater solid	$1.59 \times 10^{-1}$	5.10		
<u>Shot 2</u>				
Crater liquid	$1.65 \times 10^{-1}$			
Able solid	$7.50 \times 10^{-3}$		$8.02 \times 10^{-3}$	$8.06 \times 10^{-1}$
<u>Shot 3</u>				
Victor solid	$1.54 \times 10^{-1}$	1.84	$5.95 \times 10^{-2}$	$9.00 \times 10^{-1}$
Victor aqueous	10.5	9.09	4.10	11.7
Victor emulsion	$6.89 \times 10^{-1}$	$2.6 \times 10^{-1}$	$2.38 \times 10^{-1}$	

## CHAPTER 5

### DISCUSSION

#### 5.1 DISCUSSION OF ERRORS

The statistical errors in the counting rates have been minimized whenever possible by reading the activities at specified times from smooth decay curves. The omission of a self-absorption - self-scattering correction in the reduction of the analytical data for  $\text{Sr}^{89}$ ,  $\text{Zr}^{95}$ ,  $\text{Ba}^{140}$ , and  $\text{Ce}^{144}$  has introduced additional errors. The maximum possible variation, or spread, in the data that this omission can produce is 9.5 per cent for  $\text{Sr}^{89}$ , 4.6 per cent for  $\text{Zr}^{95}$ , 2.7 per cent for  $\text{Ba}^{140}$ , and 10 per cent for  $\text{Ce}^{144}$ . These maximum percentages were calculated by taking the difference between the extreme self-absorption-self-scattering corrections for all the samples and dividing by the average of these two corrections. The self-absorption-self-scattering corrections were estimated from the data presented by Engelke et al.<sup>18/</sup> In all cases the errors among the four aliquots of any one sample are much smaller than the maximum possible error presented here.

These two sources of errors are combined in the estimate of the total error for each analysis. These estimates are reported as spreads in Table 5.1. As in the calculation of the maximum possible error due to self-absorption - self-scattering effects, the

$$\text{spread} = \frac{\text{highest value} - \text{lowest value}}{\text{average value}} \times 100$$

In general the spreads are approximately twice the standard deviations. In the calculations of the R-values the spreads are compounded by the equation

$$S_R = (S_1^2 + S_2^2 + S_3^2 + S_4^2)^{1/2}$$

where  $S_R$  = Spread of the R-value

$S_1, S_2, S_3,$  and  $S_4$  = the spreads of the individual analyses for the nuclides in question (Cf. definition of R-value section 4.1)

TABLE 5.1 Per Cent Spreads of all Radiochemical Analyses

Sample	Per Cent Spread					
	Zr95	Sr89	Mo99	Ba140	Ce144	Ca45
<u>Shot 1</u>						
<u>Particle Size</u>						
<u>in <math>\mu</math></u>						
5.08	4.10	11.1	1.14	6.41	13.5	0.85
10.3	12.2	8.68	6.04	3.82	1.35	50
23.3	12.7	5.43	13.7	0.0	10.4	44
29.5	5.22	14.2	14.9	16.6	1.18	13
43.7	7.38	4.77	2.38	5.55	11.5	4.2
62.4	10.3	5.22	5.84	16.0	4.65	10
70.5	6.70	2.78	8.61	5.38	8.02	22
85.5	12.4	9.04	8.39	6.30	3.45	38
113		3.26	9.57	4.76	6.38	8.4
116		9.00	2.46	29.1	0.512	14
172		31.1	9.55	5.38	5.45	18
215			4.16	12.6	4.51	
239		1.60	8.61	23.2	6.76	
>300		10.9	24.0	3.74	24.9	
Fox solid	12.5	16.3	5.02	18.0	13.4	
Victor solid	0.613	4.06	1.77	4.72	6.58	
Crater solid	31	11.4	3.65			
Crater liquid	5.0		8.70			
<u>Shot 2</u>						
Crater liquid		6.98	5.65			
Able						
Ground sample	1.29	27.6	3.70	1.56		
<u>Shot 3</u>						
Victor solid	39.3	4.51	21.4	14.3	2.36	
Victor liquid	40.0	11.1	5.74	5.81	21	
Victor emulsion	17.5	7.89	4.50	4.44		
<u>Shot 4</u>						
<u>Time of sample</u>						
<u>collection after</u>						
<u>shot (hours)</u>						
1.5 - 3		20.8	4.13	6.31	7.58	
3.5 - 3		8.62	15.6	10.1	12.9	
8 - 9		2.95	5.12	0.73	3.93	
9 - 10		10.7	11.1	2.51	9.23	
10 - 11		8.06	7.09	4.96	50	
11 - 12		2.16	4.30	35.7	3.70	

In the calibration of the counting equipment to yield disintegration rates, calculations were performed involving the flux of a thermal neutron irradiation of  $U^{235}$  and the fission yields of pertinent nuclides from the resultant fission of the  $U^{235}$ . If the neutron flux and fission yields are each assigned a precision of 10 per cent, the microcurie values have an additional error of about 14 per cent independent of the analytical procedure.

All but two of the  $Zr^{95}$  analyses performed on the size-separated samples at early times after shot had to be repeated because of wide variations in results. Better reproducibility was obtained when the analyses were made 8 months later. There appeared to be poor exchange between carrier and tracer in the early analyses because almost identical chemical yields among the aliquots produced significantly different activities. Similar anomalous behavior of tracer zirconium has been observed in these laboratories during other investigations. The poor spreads in the  $Ca^{45}$  analyses can also be attributed to poor exchange properties between the carrier and tracer. This characteristic of  $Ca^{45}$  has also been reported by Jacobs and Jordan. <sup>19/</sup>

The  $Ba^{140}$  contamination of the sodium analyses has never been resolved. Repeated attempts to simulate the test shot samples have never reproduced this barium contamination in the sodium fraction of the cation elution. No satisfactory explanation can be offered for this anomalous behavior of barium which has been observed only in these shot samples.

## 5.2 EVALUATION OF SIZE SEPARATION AND AUTORADIOGRAPH TECHNIQUES

There are certain inherent difficulties in any method of particle size separation. Standard sieves are quite satisfactory for discrete, spherical particles, although the size fractions obtained show a considerable distribution of sizes on account of variations in the spacing of the screens. If the particles are irregular in shape, they may pass through the screens in various orientations so as to produce very broad distributions. Frangible or agglomerated particles may be broken up by the agitation necessary to carry out the separation. These factors are greatly influenced by the length of time the sieves are shaken. This time was kept to a minimum in order to minimize these effects. Nevertheless the size distributions were quite broad and did not compare well with the sieve sizes, as may be seen in Table 5.2.

TABLE 5.2

## Predicted vs Observed Particle Size Separations by Standard Sieves

Size Range of Sieves ( $\mu$ )	$d_v$ ( $\mu$ )	Number of Particles Counted
44-53	62.4	321
53-62	85.8	228
62-74	70.5	327
74-88	113	369
88-105	116	150
105-125	172	181
125-149	215	381
149-177	239	186

The fraction from the 62-74  $\mu$  sieve had a particularly broad distribution, so that all data associated with it should be viewed with great suspicion.

The Roller analyzer, used here for particles smaller than 50  $\mu$ , provides sharper size separations less sensitive to particle shape than the sieves. On the other hand it is more likely to break up fragile or agglomerated particles. A comparison of calibrated size with observed size is given in Table 5.3.

TABLE 5.3

## Predicted vs Observed Particle Size Separations by Roller Analyzer

Calibrated Size Range ( $\mu$ )	$d_v$ ( $\mu$ )	Number of Particles Counted
0-5	5.08	443
5-10	10.3	743
10-20	23.3	376
20-30	29.5	1089
30-40	43.7	429

From recent autoradiographic studies it has been found that the experimental determination of the per cent active particles in the lower size range may require a correction under certain conditions.\* This results from experimental limitations as to the size and specific activity of a particle which may be detected as hot.

\*This discussion of autoradiograph errors is due to Mr. Robert J. French of these Laboratories.

The detection of a particle as hot depends upon the number of silver grains exposed in the film, and the determining factor in such a measurement is the total flux (radiation per unit area of observation per unit time). This is a function of the activity concentration and of the particle size, shape, i.e.,

$$\text{Flux} = K A_m(R) V(R) G(R) E$$

K = constant of proportionality

$A_m(R)$  = activity concentration which may vary with size

$V(R)$  = volume ( $4/3 \pi r^3$ )

$G(R)$  = geometry factor (inverse square law for spherical particles and isotropic radiation)

E = correction factor used to express the portion of the energy distribution of beta particles to which the film is sensitive

As the limit of detection is reached, the percentage of hot particles detected will decrease from 100 to 0. This variation is to be expected since the experimental methods of detecting, the process of radioactive decay, and the exposure of developing centers of a film are all statistical in nature. This effect will be sudden or gradual (with variation in flux), depending on the statistical spread, which may be quite large. It is then necessary to make a correction for the detection efficiency (percentages of hot particles detected) in the range where this effect is present.

Because of the delay before the processing of the samples under consideration, the activity concentration may be low enough that this effect will be observed. At the time the autoradiographs were made, the activity concentration was estimated to be about 0.15  $\mu\text{c}/\text{mg}$ . It was found with artificial hot  $\text{Sr}^{90}\text{Cl}_2$  particles that the point of 50 per cent detection efficiency was at about 10 microns for a specific activity of 0.005  $\mu\text{c}/\text{mg}$ . Two considerations make these figures comparable. The fission products have a considerably higher mean energy than  $\text{Sr}^{90}$  and therefore proportionately less will be registered by this film. The  $\text{Sr}^{90}\text{Cl}_2$  crystals were very flat and would have a much smaller geometry correction than spherical particles. The flux will then increase much faster with particle size, so that a smaller particle will be detected as hot. The fallout particles in the range under consideration are essentially spherical. Therefore, the effect under consideration may result in a variation in detection efficiency from 100 per cent as the particle size decreases, which would have to be corrected for.

### 5.3 VARIATION OF RADIOCHEMICAL COMPOSITION WITH PARTICLE SIZE, ZERO POINT ENVIRONMENT, AND TIME AND DISTANCE OF COLLECTION

The variation of radiochemical composition with particle size is illustrated graphically in Fig. 5.1 - 5.7. The activity concentration decreases regularly with particle size to about 50  $\mu$ ; above 50  $\mu$  the situation is somewhat obscure. Figs. 5.1, 5.3, and 5.4 exhibit a sharp discontinuity at 50  $\mu$ . It is possible to draw lines through the points in the other figures in such a manner as to indicate discontinuities, rather than the smooth curves shown. It has been postulated<sup>20/</sup> that this discontinuity is related to the breaking up of agglomerates by the Roller analyzer, as discussed in the preceding section.

The differences between the various curves detail the fractionation indicated by the R-values (Tables 4.3). Only the relationships between the different curves can be regarded as significant, however because of the uncertainty in the per cent active particles mentioned in the preceding section. In another report<sup>21/</sup> the authors have used certain assumptions regarding  $\text{Ca}^{45}$  to obtain per cent active particles figures. Correction of the data by these figures leads to curves whose slopes have been interpreted to give an insight into the mechanism of particle formation.

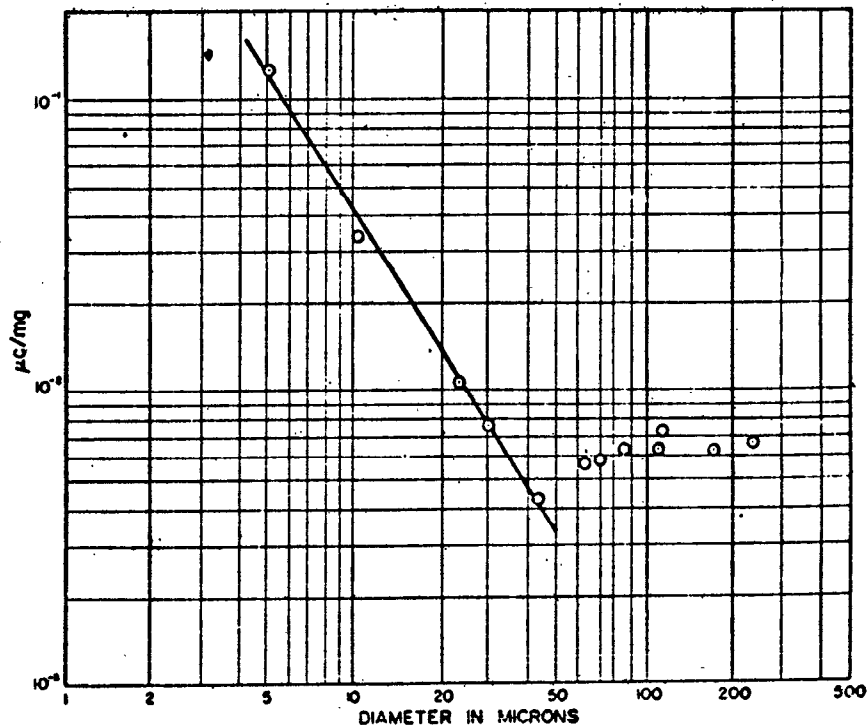


Fig. 5.1 Activity Concentration of  $\text{Sr}^{89}$  vs Particle Size

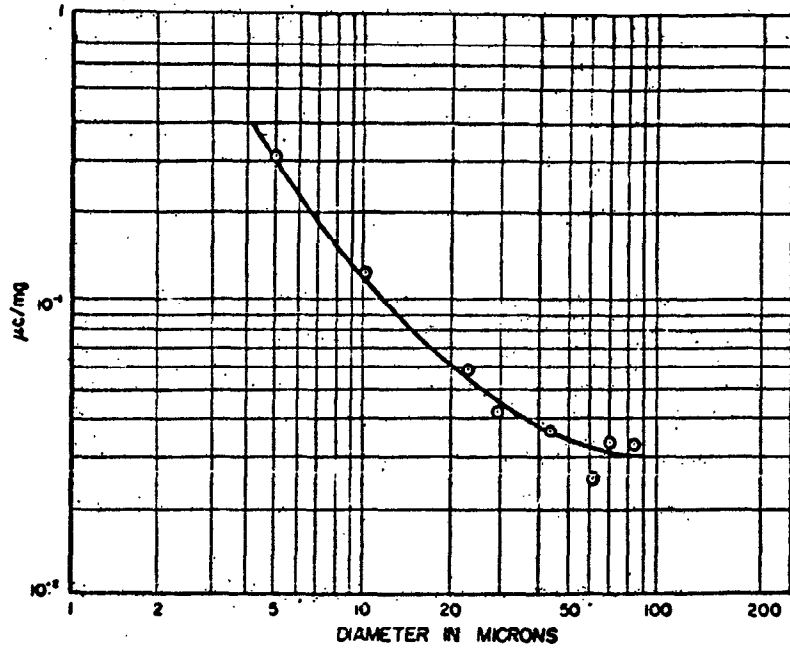


Fig. 5.2 Activity Concentration of Zr<sup>95</sup> vs Particle Size

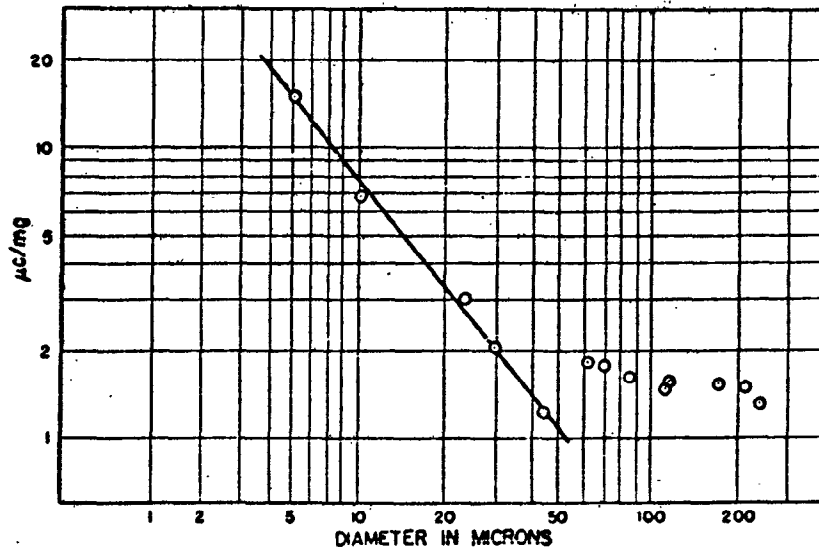


Fig. 5.3 Activity Concentration of Mo<sup>99</sup> vs Particle Size

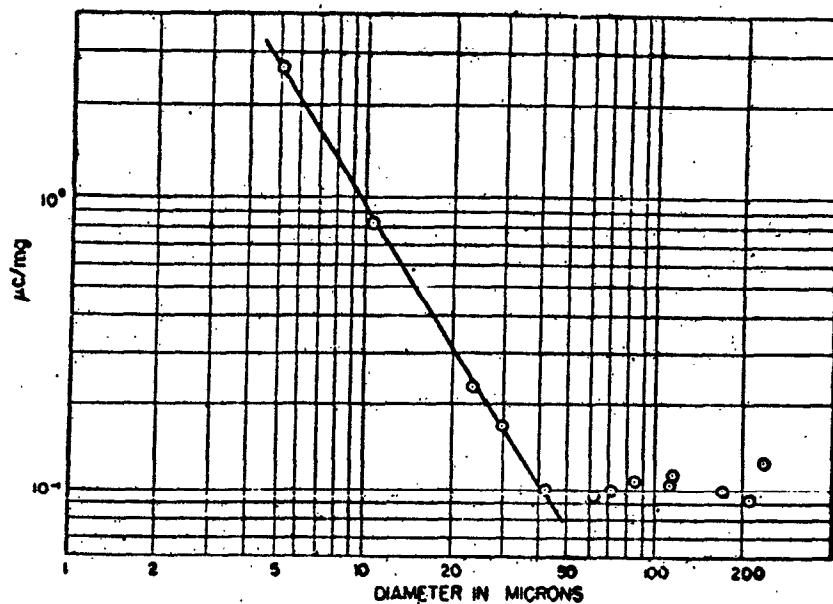


Fig. 5.4 Activity Concentration of Ba<sup>140</sup> vs Particle Size

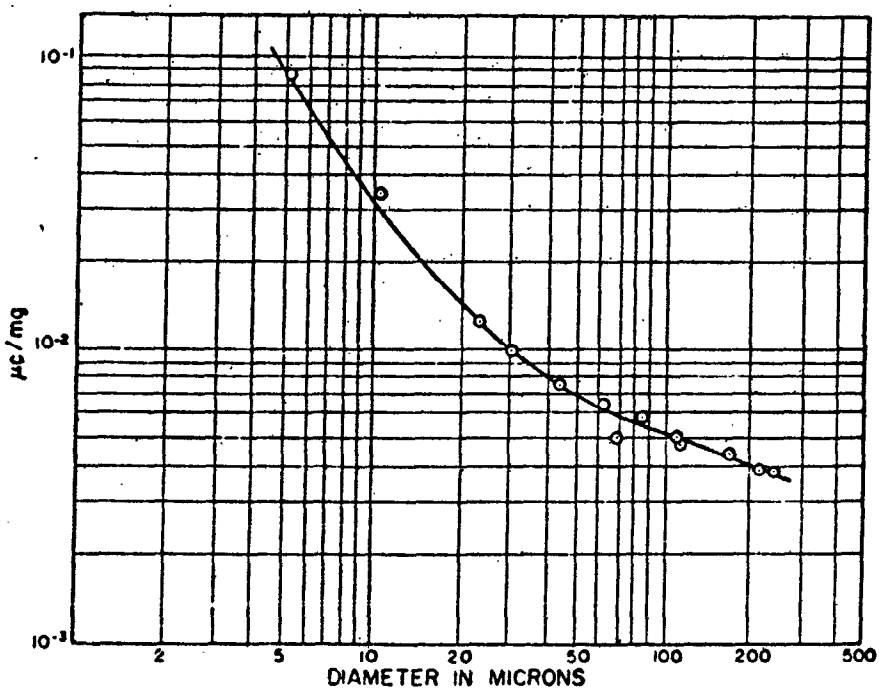


Fig. 5.5 Activity Concentration of Ce<sup>144</sup> vs Particle Sizes

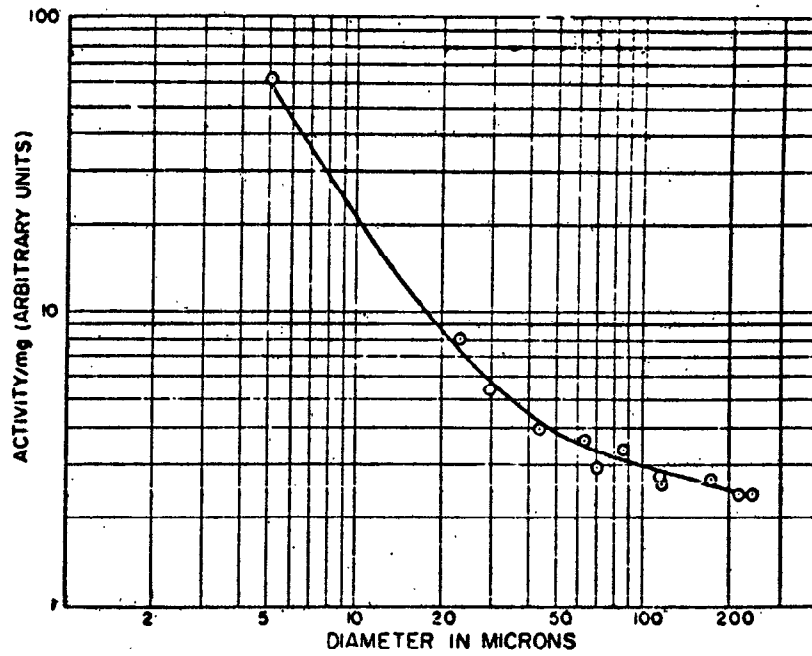


Fig. 5.6 Gross Activity Concentration vs Particle Size

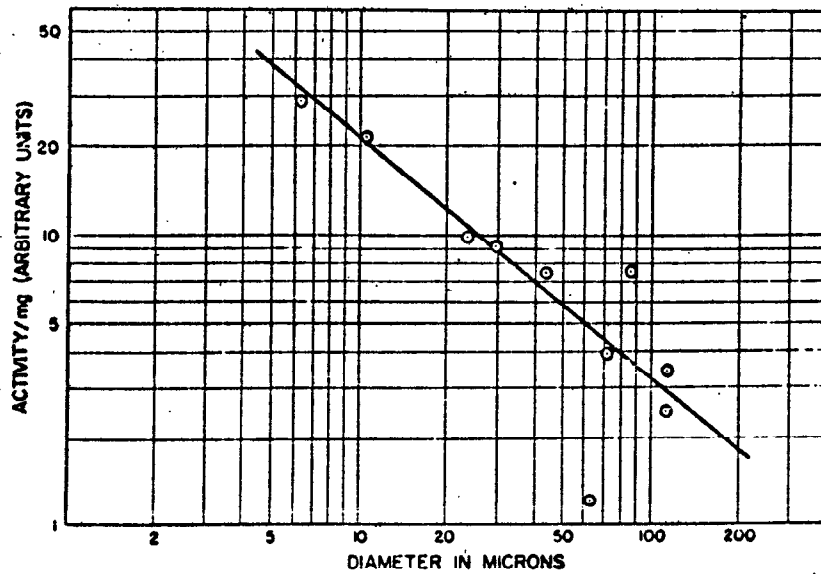


Fig. 5.7 Activity Concentration of Ca<sup>45</sup> vs Particle Size

Insufficient data were obtained to study the effect of zero point environment adequately. It was found that the surface land shots produced predominantly solid fallout, while the surface water shots produced predominantly liquid fallout. Iron was found in fallout from one of the barge shots.

Tables 4.6 and 4.7 show that the gaseous precursor nuclides,  $\text{Sr}^{89}$  and  $\text{Ba}^{140}$ , increased with time in comparison to  $\text{Mo}^{99}$  and  $\text{Ce}^{144}$ . This result can be attributed to the expected association of gaseous precursor nuclides with late condensing material. The iron from the short barge, which has no precursor, behaved like  $\text{Mo}^{99}$  and  $\text{Ce}^{144}$ .

An insufficient number of samples was obtained to find a correlation of radiochemical composition with distance. Furthermore, for such large shots the samples collected were probably not at sufficiently different distances from ground zero to show significant effects on radiochemical composition.

#### 5.4 LIQUID FALLOUT AND BASE SURGE

Beyond the fact that there was radioactive liquid fallout from Shots 1, 3, and 4, this project obtained little information of value about liquid fallout because shot delays and slow recovery permitted significant evaporation of the liquid phases, so that liquid volumes could not be determined with any accuracy.  $\text{Sr}^{89}$  and  $\text{Ba}^{140}$  showed the greatest tendency to be concentrated in the liquid fallout.

As pointed out in Section 3.1, the base surge sampling was unsuccessful. The Program Director 22/ has quoted Project 1.1c to the effect that there was no base surge of significant extent.

#### 5.5 GROSS DECAY

The slopes of the gross decay curves measured from 110 to 200 days after Bravo shot for each particle size fraction are plotted in Fig. 5.8 as a function of particle size. Below  $50 \mu$  there is a slight decrease in the gross decay rate with increasing particle size. Above  $50 \mu$  the general trend is not as clearly defined. However the entire curve resembles the activity behavior of the concentration of  $\text{Sr}^{89}$  and  $\text{Ba}^{140}$  with respect to particle size.

According to Hunter and Ballou  $\text{Sr}^{89}$ ,  $\text{Y}^{91}$ ,  $\text{Zr}^{95}$ ,  $\text{Nb}^{95}$ , and  $\text{Ru}^{103}$ ,  $\text{Ce}^{144}$ ,  $\text{Ce}^{144}$ - $\text{Pr}^{144}$  contribute approximately 90 per cent of the total activity at the time the gross decay measurements were made. The induced  $\text{Ca}^{45}$  also contributes significant activity in the fallout samples after 110 days.  $\text{Ce}^{144}$ ,  $\text{Ru}^{103}$  and  $\text{Y}^{91}$  were not analyzed but an estimate of the contributions of the first two can be made by multiplying the measured  $\text{Ce}^{144}$  concentrations by the literature  $\text{Ru}^{103}/\text{Ce}^{144}$  and  $\text{Ce}^{144}/\text{Ce}^{144}$  values for thermal fission of  $\text{U}^{235}$ . Since  $\text{Y}^{91}$  has a 9 second rare gaseous precursor,  $\text{Y}^{91}$  may behave like  $\text{Sr}^{89}$  which has a 2.6 minute rate gas precursor. Consequently the  $\text{Y}^{91}$  concentrations can be calculated from the  $\text{Sr}^{89}$  concentration and the  $\text{Y}^{91}/\text{Sr}^{89}$  literature value. If these activity concentrations are corrected for the mounting absorption of the counting rig in which the gross decay measurements were made,

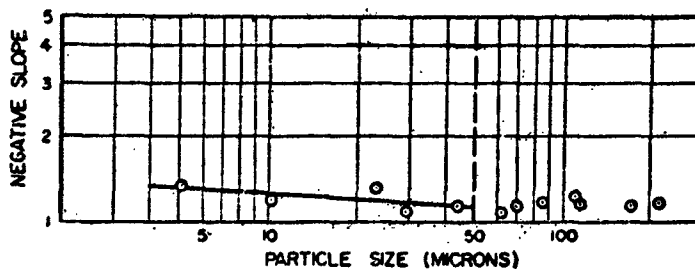


Fig. 5.8 Negative Slope of Gross Decay Curve vs Particle Size From 110-200 Days

the self-absorption, self-scattering, and back-scattering of the samples themselves, an estimate of the gross decay can be made. Such calculations yield decay rates that are slightly lower than the experimentally determined rates but they both follow the same trend with particle size below 50  $\mu$ . The discrepancies between the calculated values and the experimental values might be expected in view of the many approximations involved in the calculations. In general the slight decrease in decay rate with increasing particle size below 50  $\mu$  can probably be attributed to the relative increase in the activity concentration of  $\text{Ca}^{45}$  with respect to the other activities present. Since  $\text{Ba}^{140}/\text{La}^{140}$  behaves similarly to  $\text{Sr}^{89}$ , the variations in the gross decay rates are probably more pronounced at earlier times when the  $\text{Ba}^{140}/\text{La}^{140}$  equilibrium is a significant contributor to the total activity. The uranium capture products from Bravo shot completely masked the fission product decay characteristics for the first 30 days. Unfortunately no data were obtained between 30 and 100 days.

## CHAPTER 6

### CONCLUSIONS AND RECOMMENDATIONS

#### 6.1 CONCLUSIONS

The activity concentrations of  $\text{Sr}^{89}$ ,  $\text{Zr}^{95}$ ,  $\text{Mo}^{99}$ ,  $\text{Ba}^{140}$ , and  $\text{Ce}^{144}$  in the hot fallout particles from Shot 1 collected at How decreased regularly with increasing particle size from 5 to 50  $\mu$ . The relationships displayed a discontinuity or inflection at about 50  $\mu$ . Between 5 and 50  $\mu$  there was relative fractionation of these fission products with the exception of  $\text{Mo}^{99}$  and  $\text{Ce}^{144}$ .

Determination of the relative amounts of  $\text{Ca}(\text{OH})_2$  and  $\text{CaCO}_3$  in the samples gave inconclusive results.

The relative concentration of  $\text{Sr}^{89}$  and  $\text{Ba}^{140}$  in Shot 4 fallout increased with time of collection.

There was fallout of both radioactive solid and radioactive liquid from Shots 1 and 3.  $\text{Sr}^{89}$  and  $\text{Ba}^{140}$  displayed a greater tendency to concentrate in the liquid phase than the other fission products studied. Shot 4 fallout was almost entirely liquid.

The base surge sampling program was unsuccessful.

The gross decay Shot 1 fallout did not vary with particle size at early time. At later times the gross decay variation with particle size does correlate with the slight trend in radiochemical composition.

APPENDIX A

RADIOCHEMICAL PROCEDURES

CALCIUM

by

R. Jensen, F. Celio, and P. W. Krey

A.1 INTRODUCTION

The calcium is separated from the majority of the fission products by a palladium sulfide scavenging, a calcium carbonate precipitation, and several ferric hydroxide scavengings. Further purification is effected by several barium and strontium nitrate scavengings followed by two additional ferric hydroxide scavengings. The calcium is finally precipitated and mounted for counting as the calcium oxalate monohydrate. The chemical yield averages about 25 per cent.

A.2 REAGENTS

Ca carrier: 10 mg Ca/ml (added as  $\text{Ca}(\text{NO}_3)_2 \cdot 4\text{H}_2\text{O}$  in  $\text{H}_2\text{O}$  standardized)  
Fe carrier: 10 mg Fe/ml (added as  $\text{FeCl}_3 \cdot 2\text{H}_2\text{O}$  in dilute HCl)  
Pd carrier: 10 mg Pd/ml (added as  $\text{PdCl}_2 \cdot 2\text{H}_2\text{O}$  in dilute HCl)  
Ba carrier: 10 mg Ba/ml (added as  $\text{Ba}(\text{NO}_3)_2$  in  $\text{H}_2\text{O}$ )  
Sr carrier: 10 mg Sr/ml (added as  $\text{Sr}(\text{NO}_3)_2$  in  $\text{H}_2\text{O}$ )  
 $\text{H}_2\text{S}$  : gas  
Aerosol OT: 0.1% solution  
 $\text{NH}_4\text{OH}$  : conc.  
 $\text{K}_2\text{CO}_3$  : saturated aqueous solution  
 $\text{HNO}_3$  : fuming, conc., 6 M  
 $(\text{NH}_4)_2\text{C}_2\text{O}_4$ : saturated aqueous solution  
Ethanol : 95%  
Ethyl ether

A.3 PREPARATION AND STANDARDIZATION OF CARRIER

Dissolve 59.0 g of  $\text{Ca}(\text{NO}_3)_2 \cdot 4\text{H}_2\text{O}$  in  $\text{H}_2\text{O}$ , add 5 ml of conc.  $\text{HNO}_3$

and dilute to 1 liter with H<sub>2</sub>O. Remove a 2 ml aliquot of the solution, make the solution basic with conc. NH<sub>4</sub>OH, and dilute to 20 ml. Precipitate the calcium by adding a slight excess of saturated solution of (NH<sub>4</sub>)<sub>2</sub>C<sub>2</sub>O<sub>4</sub>. Filter on a sintered glass Gooch crucible; wash the precipitate with 10 ml of ethanol and 10 ml of ether. Suck dry on the vacuum desiccator for one hour. Weigh the precipitate as Ca C<sub>2</sub>O<sub>4</sub>.H<sub>2</sub>O

#### A.4 PROCEDURE

1. To the sample add 2 ml of calcium carrier (10mg/ml) and 10 mg of Pd and precipitate with H<sub>2</sub>S. Add 3 drops of 0.1% solution of Aerosol OT, centrifuge and discard precipitate.
2. Boil out H<sub>2</sub>S and add conc. NH<sub>4</sub>OH carefully until the solution is basic. Centrifuge and discard precipitate if the solution is not clear.
3. Heat to boiling and precipitate calcium with 2 ml of saturated K<sub>2</sub>CO<sub>3</sub>. Centrifuge and discard supernate.
4. Dissolve precipitate with 2 ml of 6N HNO<sub>3</sub> and heat to eliminate the CO<sub>2</sub>. Make the solution basic with NH<sub>4</sub>OH and dilute to a volume of 20 ml. (Note 1).
5. Add 10 mg of Fe, centrifuge, and discard the precipitate. Repeat the iron scavenging step twice.
6. To the supernate add 10 mg of Cs, heat to boiling, and precipitate the calcium with 2 ml of standard saturated K<sub>2</sub>CO<sub>3</sub>. Centrifuge and discard the supernate. Wash the precipitate with 5 ml of H<sub>2</sub>O and discard washings. Dissolve the precipitate with 1 ml of conc. HNO<sub>3</sub>.
7. Add 10 mg of Ba and 10 mg of Sr carriers to the solution and precipitate the Ba and Sr nitrates with 25 ml of cold fuming HNO<sub>3</sub> in an ice bath. Centrifuge and discard the precipitates. Add 10 mg of Ba carrier and 5 ml of cold fuming HNO<sub>3</sub> to precipitate Ba(NO<sub>3</sub>)<sub>2</sub> again. Centrifuge and transfer supernate to a 125 ml Erlenmeyer flask.
8. Boil down to 5 ml on a hot plate and transfer to a centrifuge tube. Wash the Erlenmeyer flask twice with 3 ml of H<sub>2</sub>O adding the washings to the centrifuge tube.
9. Add conc. NH<sub>4</sub>OH carefully until the solution is basic. If necessary dilute with water to 20 ml volume (note 1). Add 10 mg of Fe carrier to precipitate Fe(OH)<sub>3</sub>. Centrifuge and discard precipitate. Repeat the Fe(OH)<sub>3</sub> scavenging step.
10. Heat the supernate to boiling and add 5 ml of a saturated solution of (NH<sub>4</sub>)<sub>2</sub>C<sub>2</sub>O<sub>4</sub>. Digest in a water bath to coagulate precipitate. Filter on Whatman #40 paper; wash with 5 ml of H<sub>2</sub>O, 5 ml of ethyl alcohol, and 5 ml of ethyl ether. Dry in a vacuum desiccator for 1 hour and weigh as CaC<sub>2</sub>O<sub>4</sub>.H<sub>2</sub>O. The chemical yield is approximately 25%.

#### A.5 NOTE:

The volume of the solution at this point must be large enough to eliminate loss of calcium as the hydroxide in the ferric hydroxide scavenging step.

## SODIUM

by

G. Fulmer and B. Intorre

### A.6 INTRODUCTION

The sodium is separated from the fission products by eluting the sample from a column of colloidal Dowex-50 cation resin. The sodium fraction of this elution contains some anions which can be removed by a subsequent elution of this fraction from an anion column of Nalcite SAR resin. The sodium fraction from the anion elution is finally slurried with fine mesh Dowex-50 to adsorb all the sodium present. The resin is then filtered on Whatman #50 paper and mounted for counting. This separation was a 100 per cent chemical yield.

### A.7 REAGENTS

Colloidal Dowex-50 cation resin  
Dowex-50, cation, resin, below 400 mesh  
Nalcite SAR resin, 20-50 mesh  
HCl 0.5 N

### A.8 PROCEDURE

1. Prepare a glass column, 11 mm inside diameter, with glass wool plugging the restricted lower end. This column is filled with colloidal Dowex-50 resin slurried in 0.5N HCl to a settled bed height of  $11 \pm 0.5$  cm. Any excess resin in the column is removed by slurrying the resin with additional 0.5 NHCl and drawing the excess from the top of the column with a syringe. Then the column is conditioned by washing with 10 ml of 3 N NaCl followed by 100 ml of 0.5 N HCl. This cycle is repeated three times (Note 1).

2. A sample containing not more than 15 mg of NaCl (usually 1 to 2 ml) is added to the column after the 0.5N HCl has drained to the top of the resin bed. Care is taken to add the sample directly to the top layer of the resin without contacting the sides of the column. After the sample has drained to the top of the resin, sufficient 0.5N HCl is carefully pipetted onto the resin to prevent slurring when the 0.5 N HCl reservoir is connected.

3. After the 0.5N HCl reservoir has been connected, the elution flow rate should be approximately 1.5 ml/min (note 2). The first 30 ml of eluate are discarded. The next 40 ml, which contain the sodium along with some anions such as molybdate, ruthenate, and, iodate, are collected for addition to an anion column.

UNCLASSIFIED

4. The anion column is composed of Malcite SAR resin, 20-50 mesh, and measures 52 cm in length and 11 mm inside diameter. It is conditioned prior to use by washing with 50 ml of 10 per cent NaOH followed by 300 to 500 ml of H<sub>2</sub>O. The fraction collected in step 3 is added to the anion column in aliquots of 10 ml, permitting the column to drain to the top of the resin bed after each addition (Note 4). The container used to collect the fraction is washed with 2 ml portions of H<sub>2</sub>O, and the washings are added to the column.

5. A distilled H<sub>2</sub>O reservoir is connected to the anion column and a flow rate of 1.0 to 1.5 ml/min is maintained. The first 15 ml of eluate are discarded. The next 70 ml containing the sodium are collected.

6. The 70 ml fraction is transferred to a beaker which contains 70 mg of fine mesh Dowex-50 (not colloidal). The slurry is stirred intermittently for 20 to 30 minutes to adsorb all the sodium on the resin.

7. The resin is filtered on Whatman #50 paper, washed with 10 ml of ethanol and 10 ml of ether, and sucked dry on a vacuum line. The resin is then mounted on an aluminum plate for counting (Note 5).

#### A.9 NOTES

1. Conditioning may be carried out using large batches of resin rather than treating the analytical columns separately.
2. The flow rate was initially restricted to 0.5 ml/min but the increase to 1.5 ml/min had no adverse effects.
3. Prior to making up the anion column, the resin can be slurried with a dilute solution of phenolphthalein. The phenolphthalein is absorbed on the resin and indicates when the resin is in the hydroxide form.
4. A much better practice is to boil the cation fraction down to a few ml before addition to the anion column.
5. The chemical yield is 100 per cent.

UNCLASSIFIED  
RESTRICTED DATA

UNCLASSIFIED

APPENDIX B

CALIBRATION OF THE ROLLER ANALYZER

by

Frank Celio

B.1 INTRODUCTION AND SUMMARY

The Roller particle size analyzer,\* Fig. B.1, was used to separate the particles under study. The Roller analyzer was used for the particle size separation of coral ( $\text{CaCO}_3$ , density 2.3 g/cc) in the 0-44  $\mu$  range. The Roller analyzer and the calibration curves in the instruction manual are designed for the size separation of spherical particles. Since the coral in question was not spherical, it was necessary to calibrate the instrument for the coral. Separation was achieved experimentally with favorable and usable results in the following ranges: 0-5, 5-10, 10-20, 20-30, and 30-40  $\mu$ .

B.2 OPERATIONAL FUNCTION

1. The air is pumped from the air compressor to an oil filter and then proceeds to the capillary flowmeter where the proper rate of flow is selected.
2. Three paper thimble filters connected in parallel are used to remove any impurities in the air.
3. The air passes through the Laboratory Lectrodryer\*\* (an activated alumina system) in which it is dried to 3 per cent relative humidity at room temperature.
4. A Drierite train is next in the system. When it turns a pinkish color, the Lectrodryer must be reactivated.
5. The air is passed through the humidifying solution, which gives it a 25 per cent relative humidity at room temperature.
6. It then passes through a water trap and flows directly to the sample in the glass tube.

\*An Instrument for particle size separation made by the American Instrument Company, Silver Spring, Maryland

\*\*Manufactured by the Pittsburgh Lectrodryer Corporation, Pittsburgh, Pennsylvania

51  
UNCLASSIFIED  
SECRET RESTRICTED DATA  
UNCLASSIFIED

**UNCLASSIFIED/UNLIMITED**

**PLEASE DO NOT RETURN  
THIS DOCUMENT TO DTIC**

---

**EACH ACTIVITY IS RESPONSIBLE FOR DESTRUCTION OF THIS  
DOCUMENT ACCORDING TO APPLICABLE REGULATIONS.**

**UNCLASSIFIED/UNLIMITED**